

## Pt-Fe NUGGETS FROM ALLUVIAL DEPOSITS IN EASTERN MADAGASCAR

THIERRY AUGÉ AND OLIVIER LEGENDRE

Groupement de Recherche "Métallogénie et Matériaux Minéraux", BRGM-CNRS, Université d'Orléans,  
1A, rue de la Férellerie, 45071 Orléans Cedex 2, France

### ABSTRACT

Pt-Fe nuggets from alluvial deposits in eastern Madagascar are rounded and range in size from 0.1 to 1 mm; they all consist of isoferroplatinum, with extensive substitution of other platinum-group elements (PGE) for Pt and Cu for Fe. Isoferroplatinum nuggets contain a large variety of inclusions of silicates, glass and platinum-group minerals. Primary silicates consist of K-feldspar, plagioclase, clinopyroxene and amphibole. The included glass is rich in Si and Al, with a high content of alkalis. Two kinds of platinum-group minerals (PGM) are included in nuggets: trapped pre-existing phases, and PGM resulting from the crystallization of PGE-rich droplets trapped in a liquid state. The first type consists of Os-rich alloy, laurite, erlichmanite, cooperite, braggite, kashinite, hollingworthite, keithconnite and iridium oxide. The second type comprises Os alloy and keithconnite, and eight unnamed phases dominated by complex Pt, Pd, Rh, Cu, Ni sulfides. Evidence of exsolution of osmium and unmixing of Pt<sub>3</sub>Cu and Pt<sub>3</sub>Fe end members from an original Pt<sub>6</sub>CuFe composition also has been recognized. The nuggets crystallized at magmatic conditions and evolved very little after their crystallization. They derive from a medium enriched in Pt, with variable amounts of Pd. The presence of other PGE is reflected in the nature of the included PGM and in the composition of the nuggets. Local variations in oxygen fugacity during formation of the PGM have been observed; the absence of base-metal sulfides and the scarcity of the PGE sulfides indicate a low fugacity of sulfur. The presence of silicate and glass inclusions suggest that isoferroplatinum crystallization could have been influenced by coexistence of two different magmas. An Alaskan-type complex is a potential source for these nuggets.

*Keywords:* platinum-group minerals, platinum-group elements, nuggets, placers, electron microprobe, Madagascar, unnamed platinum-group minerals, iridium oxide, silicate inclusions, glass inclusions.

### SOMMAIRE

Des pépites d'alliage Pt-Fe provenant d'alluvions situées sur la côte Est de Madagascar ont été étudiées. Leur taille varie entre 0,1 et 1 mm. Dans tous les cas, il s'agit d'isoferroplatine présentant des substitutions importantes des autres éléments du groupe du platine (EGP) au Pt d'une part et du Cu au Fe d'autre part. Ces grains d'isoferroplatine contiennent une grande variété d'inclusions, comprenant des silicates, une phase vitreuse et des minéraux du groupe du platine (MGP). Les silicates primaires rencontrés sont feldspath potassique, plagioclase, clinopyroxène et amphibole. Le verre est une phase riche en Si, Al et en alcalins. Parmi les inclusions de MGP rencontrées, on distingue celles correspondant à des minéraux piégés à l'état solide et celles qui résultent de la cristallisation de gouttelettes d'EGP, piégées à l'état liquide. Les premières comprennent: alliage riche en Os, laurite, erlichmanite, coopérte, braggite, kashinite, hollingworthite, keithconnite et un oxyde d'Ir. Les secondes, mis à part un alliage riche en Os et la keithconnite, comprennent huit différents minéraux correspondant à des phases inconnues du système Pt, Pd, Rh, Cu, Ni, S. Une texture d'exsolution impliquant l'Os et la séparation de phases de type Pt<sub>3</sub>Cu et Pt<sub>3</sub>Fe à partir d'un terme initial Pt<sub>6</sub>CuFe ont également été observées. L'ensemble des caractéristiques des pépites indique qu'elles ont cristallisé dans des conditions magmatiques et ont subi peu de transformations ultérieures. Elles proviennent d'un milieu enrichi en Pt, avec des teneurs variables en Pd. La présence des autres EGP dans le système est indiquée par la nature des MPG inclus et par l'ampleur des substitutions impliquant les EGP. Des variations locales de la fugacité en oxygène auraient été importantes lors de la cristallisation. L'absence de sulfure de métaux de base et la nature des sulfures d'EGP inclus témoignent d'une faible fugacité en soufre. La nature des phases silicatées incluses suggère que la cristallisation de l'isoferroplatine pourrait avoir été influencée par la coexistence de deux magmas de composition différente. Il est possible que l'origine des pépites soit à rechercher dans une formation du type "complexe alaskéen".

*Mots-clés:* minéraux du groupe du platine, éléments du groupe du platine, pépites, gravier alluvionnaire, microsonde électronique, Madagascar, minéraux du groupe du platine sans nom, oxyde d'iridium, inclusions de silicates, inclusions vitreuses.

## INTRODUCTION

Alluvial platinum has been known in Madagascar since the early part of the century. Platinum was exploited as a by-product of gold from two small placers in the Anosibe Antanambao – Manampotsy region (about 120 km southeast of Antananarivo; Fig. 1). From these two sources, 459 g of Pt was collected, but the exact production of each placer is not known. Much later (1959–1960), geological mapping indicated the presence of ultramafic rocks in the vicinity of the platinum-bearing placers. This observation initiated an exploration program for Ni and Pt possibly related to large mafic–ultramafic bodies.

Thus, the Anosibe region, where the first placer, Ambodivolafofotsy, is situated, was systematically prospected. Two thousand alluvial concentrates were made, but no platinum-group mineral was recognized. However, the study of the other prospect (Antanambao–Manampotsy), which includes the second placer (Ambodibonara, Fig. 1) was more encouraging; regional alluvial prospecting revealed platinum-group minerals (PGM) in several rivers, but interest in the Ambodibon-

ara placer was not sustained. In both cases, however, the content of PGM did not attain economic concentrations.

Recent interest devoted to platinum-group elements (PGE) in this region led us to examine the earlier findings in greater detail. Through the kindness of a BRGM prospector, who provided us two concentrates, we have studied the mineralogy of these alluvial minerals.

## GEOLOGICAL SETTING

The most recent geological study available concerning this rather inaccessible region of the eastern coast of Madagascar was completed in 1962 (J. Conraux, unpublished BRGM report). In this area, four rock units have been distinguished; they are all part of the Archean shield and have been metamorphosed to the granulite facies:

1. The Ambinanindrano Group includes weakly migmatized ortho- and paragneisses, quartzite, gabbro, dolerite and basalt dykes. Lenses of ultrabasic rocks also are present.
2. The Niarovana–Mahela Group consists of gneiss,

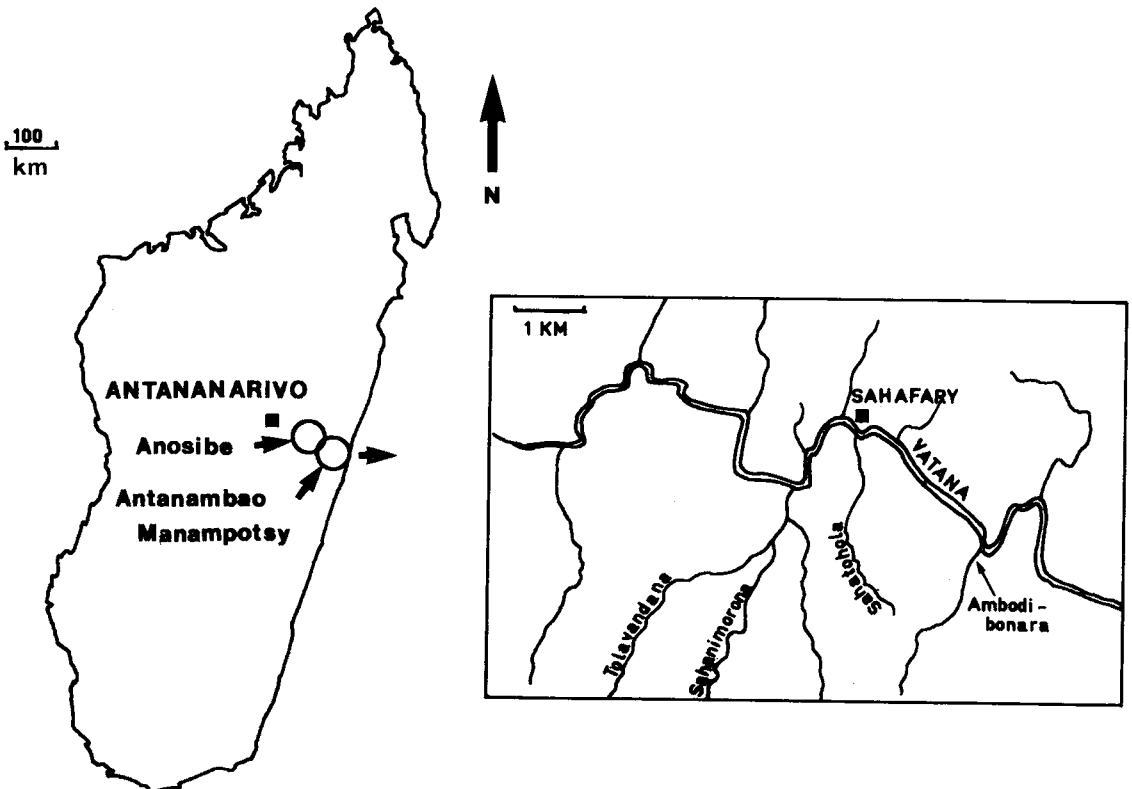


FIG. 1. Location of the Anosibe and Antanambao–Manampotsy areas in Madagascar. Area shown in detail corresponds to the Ambodibonara–Sahafary sector.

charnockite and granite, with "cores" of peridotite and pyroxenite in places.

3. The Antanambao-Manampotsy Group is a large unit that has been intensively "granitized" and includes quartzofeldspathic granulite, charnockite, gneiss and rare basic "enclaves".

4. The Ambodibonara Group is mainly composed of amphibole-rich gneiss. This unit comprises metamorphosed layered gabbro massifs, with ultramafic horizons, one of which is continuous over a distance of about 6 km. According to Conraux (1962), this group shows the highest concentration of ultramafic lenses.

Three ultramafic facies exist, and they represent possible sources of alluvial PGM:

1. Pyroxenites, locally containing olivine, occur as small isolated lenses or interlayered with gabbro. In the former occurrences, the pyroxene is enstatite, whereas in the latter occurrences, the pyroxene is more enriched in Fe.

2. Peridotite and serpentinite. This facies is rare and occurs either as isolated boulders in areas of gabbroic rock, or in association with the pyroxenite lenses described above. Fresh rocks are composed of lherzolite and harzburgite, with 20–30% olivine.

3. Tremolite and soapstone, the two most common forms of ultramafic rocks, may have been derived from peridotite and pyroxenite. They occur as isolated lenses 1 to 3 m thick and 10 to 30 m long, that are invariably concordant with respect to the regional foliation.

#### PROSPECTING TECHNIQUES AND RESULTS

The search for alluvial PGM has been conducted in two areas and involved two stages. The first area (Anosibe: Henry 1962) includes the Ambodivolafofity placer, and the second (Antanambao-Manampotsy), the Ambodibonara placer (Fig. 1). The first stage consisted in collecting heavy-mineral concentrates from river gravel, with a sampling density of about one concentrate per km<sup>2</sup>. This approach revealed no potential for the Anosibe region. Similarly, a more detailed study of the Ambodivolafofity placer showed no significant concentration of the PGM in the sediment.

The regional study of the second prospect (Antanambao-Manampotsy) defined a PGM-rich region (Ambodibonara-Sahafary) that includes the PGM-rich placer previously exploited, and alluvium from three other rivers. The second stage consisted in digging a series of reconnaissance pits in the gravel of PGM-rich flats (200 – 300 m apart) in the anomalous sectors previously defined. In those zones where the highest PGM content was obtained, lines of more closely-spaced pits were dug.

Gravel and the upper part of the bedrock exposed in the pit were then panned. The volume of material washed varied between 100 and 3000 liters. The PGM, described

as being "as easy to recognize in the pan as gold nugget" (Conraux 1962), were hand-picked, and the PGE content of the gravel roughly estimated.

The work of Conraux (1962) was very detailed on the Ambodibonara flat, where remains of the old working were recognized. Unfortunately, a very low content of PGE was obtained. Three other sectors were selected for detailed work: the *Sahatoloha River*, where of the 12 pits dug, eight gave positive results and defined a weakly mineralized zone 200 m long and 100 m wide; the *Sahanimorona River*, where three pits out of 14 gave positive results, and the *Tolavandana River*, where 21 pits were prepared and PGM were found in 16 pits, which delimited a mineralized flat 400 m long and 100 m wide. The mineralized gravel layer is 70 cm thick and covered by 1 to 3 m of overburden. In spite of the fact that this flat gave the highest concentration of the PGM, it is of little economic interest.

During this project (Conraux 1962), a total of 70 pits were made, and about 900 PGE nuggets were collected. However, only two concentrates were studied, both from pits made in the same flat of the Tolavandana River. From the first pit (P1), where 700 liters of gravel were panned, 25 PGE nuggets and 15 gold particles were collected. From this concentrate, ten grains of magnetite, ten of ilmenite, and only nine PGE nuggets were obtained. In the second pit (P2), 1100 liters were washed, and 38 PGE nuggets and 20 gold nuggets collected. Minerals that we obtained from this concentrate consist of one grain of magnetite, nine of ilmenite, one particle of gold, and only 24 PGE nuggets.

#### ANALYTICAL TECHNIQUES

The PGM were examined by scanning electron microscopy (SEM) in order to study their morphological characteristics, and were then mounted in resin to prepare polished sections for the examination under reflected light. SEM was again used to observe small inclusions occurring in the PGM, and a Si-Li energy-dispersion spectrometer was employed for qualitative analysis of the various inclusions.

In a second stage, PGM and their inclusions were analyzed quantitatively with a Cameca "Microbeam" electron microprobe under the following conditions: acceleration voltage 25 kV, beam current 15 nA, counting time 6 seconds. Pure metals were used as standards except for S and As, where pyrite and GaAs were utilized. The following X-ray lines were used: OsL $\beta$ , IrL $\alpha$ , RuL $\alpha$ , RhL $\alpha$ , PtL $\alpha$ , PdL $\beta$ , AuL $\alpha$ , TeL $\alpha$ , AsL $\beta$ , SK $\alpha$ , FeK $\alpha$ , NiK $\alpha$ , CuK $\alpha$ . A ZAF correction program was used, and minor corrections were made for interferences of RuL $\beta$  and RhL $\alpha$ . Other elements, such as Bi or Sb, were not detected. Silicates were analyzed using a routine program (acceleration voltage 15 kV, beam current 12 nA, counting time 6 seconds).

## SAMPLE DESCRIPTION

*Platinum nuggets*

All the PGE nuggets appear to be Pt-Fe alloy, except one nugget with a complex shape, which is a polycrys-

talline aggregate composed of euhedral crystals of a Os-Ir alloy, Ru-sulfide and silicate embedded with Pt-Fe alloy. The nuggets, which range in size from 0.1 to 1 mm, are either rounded or irregular. Some are coated by iron oxide or silicate alteration. A morphological study by SEM confirms these observations, and shows

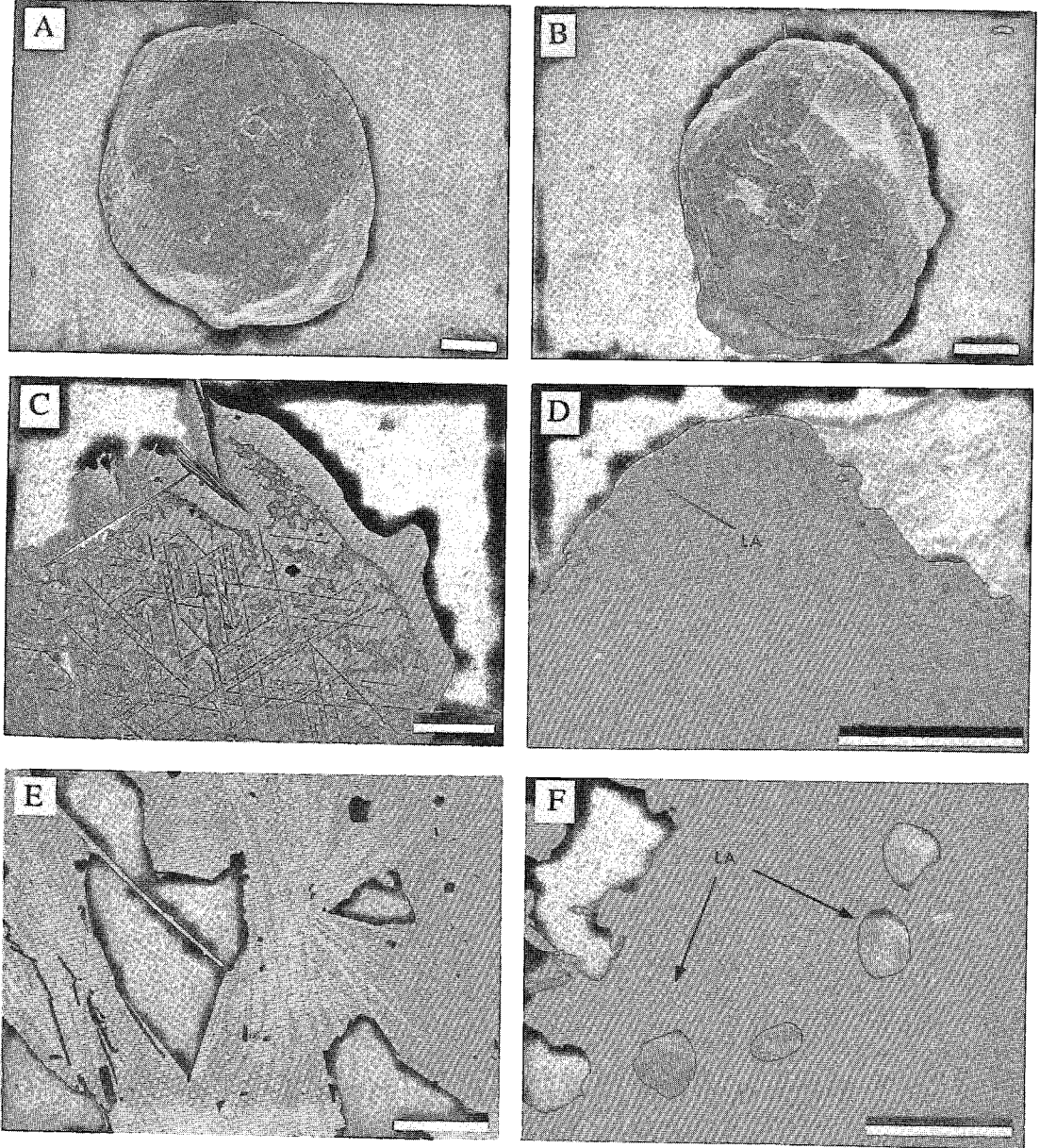


FIG. 2. Scanning electron microscope images of isoferroplatinum nuggets. A, B: images showing different aspects of the morphology of the nuggets; C: section of nugget 2G1 showing the four cleavage traces and unmixed  $\text{Pt}_3\text{Cu}$  (dark grey); D: nugget B12 showing a rim of included euhedral laurite (LA) at its periphery; E: laths of osmium in isoferroplatinum nugget (nugget B3); F: round inclusions of zoned laurite (LA, nugget B11). Scale bar is 100  $\mu\text{m}$  for A and B, and 40  $\mu\text{m}$  for other images.

in some cases perfect spherical forms either with smooth or irregular surfaces or more complex rounded forms (Figs. 2A, B).

The main interest of these nuggets resides in the proportion and composition of the inclusions they contain. Two kinds of inclusions within the nuggets have been encountered: (1) PGM, and (2) silicates (Table 1). No other mineral group (such as base-metal sulfides) has been observed as inclusions in the Pt-Fe nuggets.

#### *Inclusions of platinum-group minerals*

The PGM occurring as inclusions within isoferroplatinum consist of alloys, sulfides, sulfarsenides, tellurides, telluro-arsenides and oxides. The most common are Os-Ir-Ru alloys and members of the laurite-erlichmanite series. They vary widely in shape, from laths corresponding to flat crystals, to equidimensional crystals. The relationship to the host mineral also is variable. PGM inclusions occur as single minerals or aggregates as large as 150  $\mu\text{m}$  (Figs. 2E, F, 3A) trapped within isoferroplatinum, and as complex assemblages, apparently trapped as a single globular liquid phase. Such "globules", although small (5 to 10  $\mu\text{m}$  in diameter), may contain as many as six different minerals (Figs. 3C, D, E, F). Pt-Cu alloy (Fig. 2C) and lamellae of osmium also are developed from the isoferroplatinum by exsolution.

The distribution of the PGM included within the nuggets is variable. They correspond to: single euhedral

crystals homogeneously scattered in the nugget (Fig. 2F), and single or multiphase crystals disposed as regular rims close to the border of the isoferroplatinum nuggets, indicating that they have been trapped during nugget growth (Fig. 2D). Several nuggets are inclusion-free, whereas others may contain up to nine mineral species; most contain only one or two species (commonly Os-Ir-Ru alloy and laurite; Table 1). Composite nugget 2G5, made of laths of PGE alloys and Ru sulfide cemented by isoferroplatinum, provides good evidence of the entrapment of inclusions.

#### *Silicate inclusions*

Three types of silicate inclusions within platinum nuggets have been distinguished: (1) alteration silicates, (2) high-temperature minerals, and (3) two-phase inclusions composed of glass and silicate. Type-1 and type-2 inclusions commonly occur in contact with laths of the PGE alloy.

Inclusions of alteration minerals, the most common and the largest, are composed of kaolinite and iron hydroxides. Most are mixtures of undetermined phases. Although in some cases they seem to be isolated, they are products of supergene alteration of high-temperature minerals or cavity fillings.

Inclusions of high-temperature silicates are small and usually euhedral. Associations of amphibole + clinopyroxene and amphibole + K-feldspar have been found,

TABLE 1. LIST OF THE PGM FOUND IN THE ISO FERROPLATINUM NUGGETS

| Nuggets   | 2G1 | B2 | B6 | B13 | B11 | B3 | B12 | 2G8 | 1A4 | 1A5 | B4 | B10 | 1B3 | 2G5 | B16 | 2G3 |
|---|-----|----|----|-----|-----|----|-----|-----|-----|-----|----|-----|-----|-----|-----|-----|
| Isoferroplatinum (Pt <sub>2</sub> Fe)   | ●   | ●  | ●  | ●   | ●   | ●  | ●   | ●   | ●   | ●   | ●  | ●   | ●   | ●   | ●   | ●   |
| Osmium Os(Ir,Ru)  |     | ●  | ●  | ●   | ●   | ●  |     |     | ●   | ●   |    |     |     | ●   | ●   | ●   |
| Ir-oxide  |     |    |    | ●   |     |    |     |     |     |     |    |     |     |     |     |     |
| Laurite (RuS <sub>2</sub> )   |     | ●  | ●  | ●   | ●   | ●  | ●   | ●   |     |     | ●  | ●   |     | ●   | ●   | ●   |
| Erlichmanite (OsS <sub>2</sub> )  |     |    |    | ●   |     |    |     |     |     |     |    |     |     | ●   |     |     |
| Hollingworthite (RhAsS)   |     |    |    |     |     |    |     |     |     |     | ●  |     |     |     | ●   |     |
| Kashinite (Ir,Rh) <sub>2</sub> S <sub>3</sub>   |     |    |    |     |     |    |     |     |     |     |    |     | ●   |     | ●   |     |
| Cooperite (PtS)   |     |    |    |     |     |    |     |     |     |     |    | ●   |     |     |     |     |
| Braggite (Pt,Pd)S   |     |    |    |     |     |    |     |     |     |     | ●  |     |     |     | ●   |     |
| Keithcomite (Pd <sub>2</sub> Te)  |     |    |    |     |     |    |     |     | ●   | ●   |    |     | ●   |     | ●   | ●   |
| Pt <sub>2</sub> Cu  | ●   |    |    |     |     |    |     |     |     |     |    |     |     |     |     |     |
| 1 (Pd,Pt) <sub>3</sub> (As,Te) Vincentite   |     |    |    |     |     |    |     |     |     |     |    |     |     |     | ●   |     |
| 2 Pd <sub>2</sub> S   |     |    |    |     |     |    |     |     |     |     |    |     |     |     | ●   |     |
| 3 (Pd,Pt) <sub>2</sub> S  |     |    |    |     |     |    |     |     |     |     |    |     |     |     | ●   |     |
| 4 (Pd,Pt) <sub>3</sub> (Cu,Ni) <sub>2</sub> S <sub>2</sub>  |     |    |    |     |     |    |     |     |     |     |    |     |     |     |     | ●   |
| 5 (Rh,Ir)(Pt,Pd)(Cu,Ni) <sub>2</sub> S <sub>2</sub>   |     |    |    |     |     |    |     |     |     |     |    |     |     |     |     | ●   |
| 6 (Pd,Pt) <sub>2</sub> (Rh,Ir)(Cu,Ni) <sub>2</sub> S <sub>2</sub>                                       |     |    |    |     |     |    |     |     |     |     |    |     |     |     |     | ●   |
| 7 (Pd,Pt,Au) <sub>2</sub> Cu  |     |    |    |     |     |    |     |     |     |     |    |     |     |     |     | ●   |
| 8 (Pt,Pd,Rh,Os,Au,Cu) <sub>3</sub> S <sub>2</sub>   |     |    |    |     |     |    |     |     |     |     |    |     |     |     |     | ●   |
| PdAs  |     |    |    |     |     |    |     |     |     |     |    | ●   |     |     |     |     |
| Nuggets 1B5, 1A2, 2G1, 2G6, 2G7, B7, B9, B14 and B15 do not contain inclusions of PGM                   |     |    |    |     |     |    |     |     |     |     |    |     |     |     |     |     |
| Nuggets 1A3, 1B1, 1B2, 1B6, 2G2, 2G4, B5 and B8 only contain inclusions or exsolution of osmium alloys. |     |    |    |     |     |    |     |     |     |     |    |     |     |     |     |     |

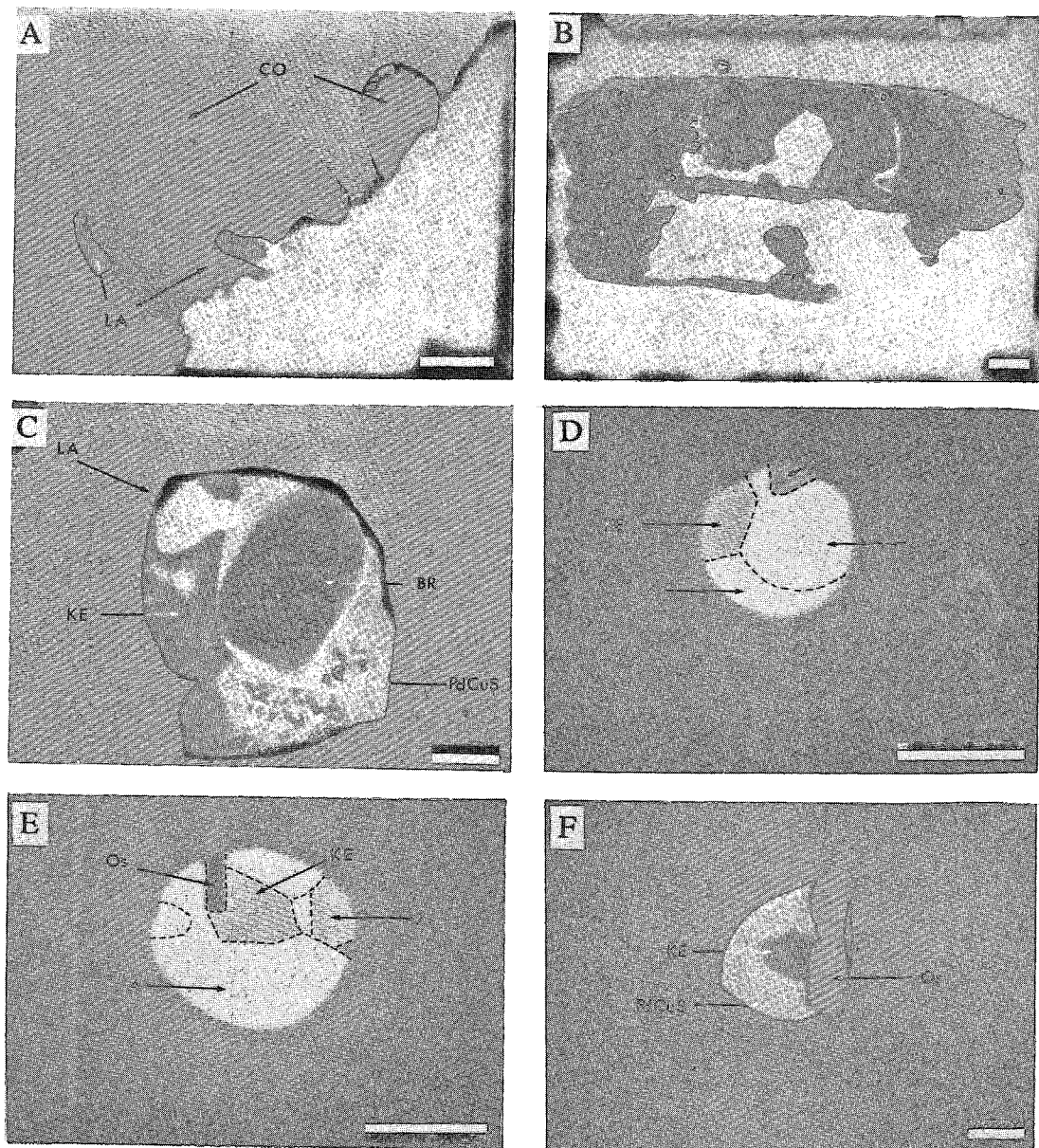


FIG. 3. Scanning electron microscope images of isoferroplatinum nuggets. A: large round crystals of cooperite (CO) with associated laurite (LA) in the isoferroplatinum nugget B10; B: zoned osmium crystal included in the nugget B11; C, D, E, F: "globules" containing different PGM included in isoferroplatinum (nuggets B16 for C, 2G3 for D, E and F). Numbers or letters on the photos refer to compositions given in text and in Table 5; PdCuS: undetermined sulfide, LA: laurite, BR: braggite, KE: keithconite, Os: osmium. Minute white inclusions on the PdCuS phase (Fig. 3C) correspond to Os alloy. Scale bar is 20  $\mu\text{m}$  for A and B, 4  $\mu\text{m}$  for other images.

whereas albite occurs as isolated inclusions. K-feldspar also occurs embedded with different PGM in composite nugget 2G5.

Composite glass-silicate inclusions also are very small (10 to 30  $\mu\text{m}$  in their largest dimensions). Of the four inclusions studied, the silicate is invariably

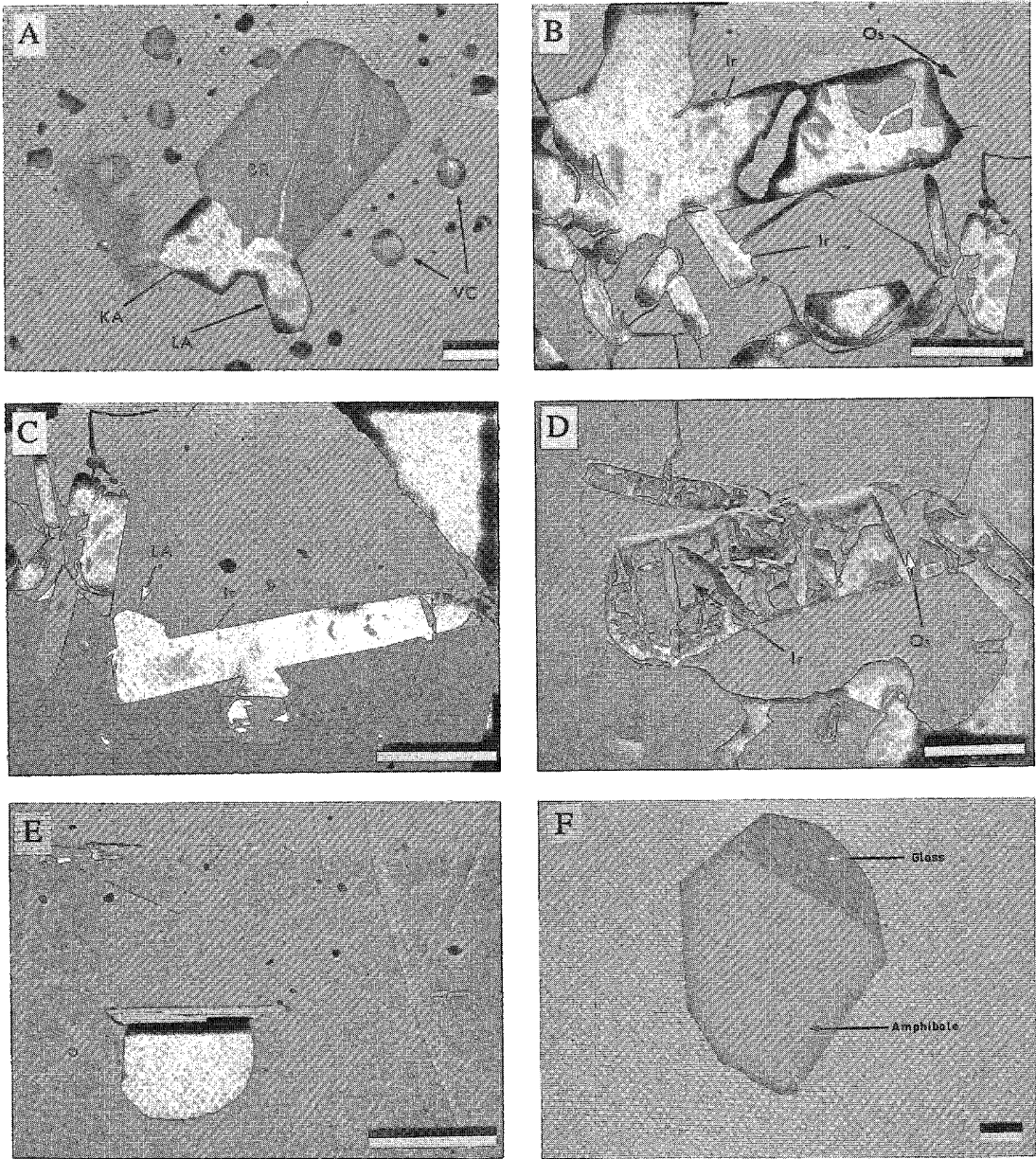


FIG. 4. Scanning electron microscope images of isoferroplatinum nuggets. A: cluster of euhedral crystals (laurite: LA, braggite: BR, kashinite: KA) surrounded by round globules dominated by vinentite, VC (nugget B16); B, C, D: different features of nugget B13 showing laths of iridium oxide (Ir), surrounded by osmium crystals (Os). Laurite is indicated by LA; E: two-phase inclusion (dark) of glass and amphibole in nugget 1A1. Note the presence of osmium laths (white); F: two-phase inclusion of amphibole (light grey) and Si-rich glass (dark grey) filling a negative crystal in isoferroplatinum (nugget 2G6). Scale bar is 40  $\mu\text{m}$ , except for A and F, where it is 4  $\mu\text{m}$ .

amphibole, with, in one case, a tiny grain of Fe-Ti oxide (probably ilmenite) and an undetermined Ca-rich phase. These inclusions are euhedral, probably

because they occupy negative PGM crystals (Figs. 4E, F).

COMPOSITION OF MINERALS  
IN THE PLATINUM NUGGETS*Isoferroplatinum*

Thirty-three PGM nuggets have been analyzed. For each grain, several point analyses have been carried out in order to test for homogeneity. No compositional zoning has been observed. In the following diagrams, results of each point analysis have been plotted for a given grain. Only representative compositions are given in Table 2. As shown in Figure 5, the whole grains have a composition close to Pt<sub>3</sub>Fe end member, corresponding to isoferroplatinum (Cabri & Feather 1975). In spite of the lack of crystallographic data necessary to characterize the Pt-Fe alloys species, the term "isoferroplatinum" will be used. The nature of elemental substitution suggests an ordered primitive cubic structure. Large variations in composition have been recorded, marked mainly by substitution of Pt for other PGE, and Fe for Cu. Substitution of Cu for Fe extends toward Pt<sub>3</sub>Cu in a phase that has been interpreted as a product of unmixing from an initial Pt-Fe-Cu composition (Figs. 2C, 5). Figure 6 shows that the Fe content of isoferroplatinum varies from 25 at.% (ideal Pt<sub>3</sub>Fe) to about 10 at.%. For the highest values of Cu, it can be seen that the

theoretical substitution is not exactly followed, and a relative deficit in Cu appears. On the other hand, the composition of the Pt-Cu phase plots slightly above the line showing the theoretical substitution, which corresponds to a slight excess in Cu. However, the composition of this phase is very close to the theoretical Pt<sub>3</sub>Cu end-member (Hansen & Anderko 1958).

The second important substitution involves Pt for Pd, with Pt decreasing from around 75 at.% (theoretical isoferroplatinum) to 62 at.%. This substitution is relatively complicated, insofar as two broad trends can be distinguished (Fig. 7). In the first, the ideal substitution is followed, from Pt<sub>75</sub>M<sub>25</sub> to Pt<sub>63</sub>Pd<sub>12</sub>M<sub>25</sub>; the second trend is marked by a deficit in Pd. The Pd - Rh correlation (Fig. 8) clearly indicates that this deficit in Pd is partly compensated by the appearance of Rh in isoferroplatinum. Two trends, one where Pd enrichment is correlated with Rh enrichment in a relationship of 2:1, and another, restricted to the highest Pd values, where the Rh content is low, appear clearly on Figure 8. The Rh-rich nuggets are interpreted to have crystallized from a medium relatively impoverished in Pd, whereas for the Rh-poor nuggets, lack of Pt was compensated by Pd-for-Pt substitution.

The role of Os, Ir and Ru in the isoferroplatinum nuggets also has been examined, since their incorpora-

TABLE 2. SELECTED ELECTRON-MICROPROBE DATA OF PLATINUM-IRON ALLOY NUGGETS

|      | B3                 | 1A1   | 1B3   | 1A5   | 1A4   | B2    | B9    | B5     | B6     | B13    | B8    | 1A3   | B15    | B14    | B10    | 1B5    | 2G1A  | 2G1B  | 2G1C  |
|------|--------------------|-------|-------|-------|-------|-------|-------|--------|--------|--------|-------|-------|--------|--------|--------|--------|-------|-------|-------|
|      | Weight per cent    |       |       |       |       |       |       |        |        |        |       |       |        |        |        |        |       |       |       |
| Pt   | 77.84              | 78.44 | 78.74 | 80.73 | 81.39 | 81.72 | 85.90 | 87.01  | 88.33  | 88.33  | 88.52 | 88.81 | 89.16  | 89.18  | 90.07  | 90.55  | 86.50 | 79.10 | 85.02 |
| Rh   | 1.82               | 1.07  | 2.72  | 1.00  | 0.47  | 1.71  | 0.35  | 0.67   | 0.83   | 0.73   | 0.93  | 0.55  | 0.45   | 0.25   | 0.13   | 0.30   | 0.45  | 0.42  | 0.44  |
| Ru   | 1.89               | 2.18  | 0.38  | 0.75  | 0.08  | 3.39  | 0.22  | 0.47   | 0.05   | 1.28   | 1.39  | 0.19  | 0.26   | 0.26   | 0.11   | 0.01   | 0.07  | 0.38  | 0.13  |
| Pd   | 3.09               | 1.92  | 4.86  | 8.44  | 6.77  | 3.24  | 1.54  | 1.29   | 1.61   | 1.19   | 1.43  | 1.90  | 0.94   | 1.04   | 1.21   | 0.03   | 1.70  | 5.02  | 2.36  |
| Ir   | 4.23               | 5.85  | 3.18  | 0.81  | 0.69  | 1.68  | 0.41  | 1.33   | -      | 1.80   | 1.47  | 0.23  | 0.12   | 0.37   | -      | 0.20   | 0.05  | 0.22  | 0.08  |
| Os   | 2.58               | 1.96  | 0.43  | 0.31  | 0.22  | 1.34  | 2.62  | -      | -      | -      | 0.04  | -     | -      | 0.03   | -      | 0.21   | -     | -     | -     |
| Au   | -                  | -     | -     | -     | 0.93  | -     | -     | -      | -      | -      | -     | -     | -      | -      | -      | -      | -     | 0.48  | 0.10  |
| Fe   | 5.68               | 7.06  | 6.99  | 3.06  | 7.65  | 3.73  | 3.75  | 8.78   | 8.37   | 5.04   | 3.86  | 6.66  | 7.23   | 7.04   | 6.41   | 8.41   | 5.61  | 1.60  | 4.81  |
| Cu   | 0.90               | 1.03  | 1.68  | 3.26  | 1.42  | 2.88  | 4.36  | 0.50   | 0.50   | 1.63   | 2.10  | 1.30  | 1.75   | 1.62   | 2.44   | 0.17   | 4.16  | 11.39 | 5.61  |
| Ni   | 0.05               | 0.05  | 0.05  | 0.05  | -     | 0.07  | 0.01  | 0.04   | 0.12   | 0.02   | 0.13  | -     | 0.01   | 0.12   | 0.00   | 0.10   | 0.05  | 0.03  | 0.03  |
| As   | 0.04               | 0.13  | 0.12  | 0.12  | 0.26  | 0.05  | 0.08  | 0.14   | 0.14   | -      | -     | 0.22  | 0.10   | 0.11   | -      | 0.19   | 0.19  | 0.23  | 0.20  |
| S    | 0.03               | 0.06  | 0.01  | 0.01  | 0.01  | 0.04  | -     | 0.04   | 0.18   | 0.07   | 0.06  | 0.02  | 0.03   | -      | 0.01   | 0.04   | 0.04  | 0.01  | 0.03  |
| Tot. | 98.15              | 99.75 | 99.16 | 98.54 | 99.89 | 99.85 | 99.24 | 100.27 | 100.13 | 100.09 | 99.93 | 99.88 | 100.05 | 100.02 | 100.38 | 100.21 | 98.82 | 98.88 | 98.81 |
|      | Atomic proportions |       |       |       |       |       |       |        |        |        |       |       |        |        |        |        |       |       |       |
| Pt   | 64.53              | 62.81 | 61.85 | 66.20 | 63.36 | 66.46 | 71.82 | 69.14  | 70.35  | 74.03  | 75.13 | 72.81 | 72.24  | 72.65  | 73.39  | 73.90  | 69.82 | 60.01 | 67.74 |
| Rh   | 2.85               | 1.62  | 4.04  | 1.55  | 0.70  | 2.64  | 0.55  | 1.01   | 1.25   | 1.17   | 1.49  | 0.85  | 0.70   | 0.39   | 0.21   | 0.46   | 0.68  | 0.60  | 0.66  |
| Ru   | 3.03               | 3.37  | 0.57  | 1.19  | 0.11  | 5.32  | 0.36  | 0.71   | 0.08   | 2.07   | 2.27  | 0.29  | 0.41   | 0.41   | 0.17   | 0.02   | 0.11  | 0.55  | 0.20  |
| Pd   | 4.69               | 2.82  | 7.00  | 12.69 | 9.66  | 4.83  | 2.36  | 1.88   | 2.36   | 1.83   | 2.22  | 2.86  | 1.40   | 1.55   | 1.81   | 0.04   | 2.51  | 6.99  | 3.45  |
| Ir   | 3.56               | 4.76  | 2.53  | 0.68  | 0.54  | 1.38  | 0.34  | 1.07   | -      | 1.53   | 1.26  | 0.19  | 0.10   | 0.31   | -      | 0.17   | 0.04  | 0.17  | 0.06  |
| Os   | 2.19               | 1.61  | 0.35  | 0.26  | 0.17  | 1.12  | 2.25  | -      | -      | -      | 0.04  | -     | -      | 0.02   | -      | 0.18   | -     | -     | -     |
| Au   | -                  | 0.08  | -     | -     | 0.71  | -     | -     | -      | -      | -      | -     | 0.09  | -      | -      | -      | -      | -     | 0.36  | 0.08  |
| Fe   | 16.45              | 19.73 | 19.17 | 8.78  | 20.80 | 10.60 | 10.96 | 24.38  | 23.29  | 14.77  | 11.44 | 19.07 | 20.45  | 20.03  | 18.26  | 23.96  | 15.82 | 4.24  | 13.39 |
| Cu   | 2.30               | 2.53  | 4.04  | 8.21  | 3.39  | 7.19  | 11.19 | 1.21   | 1.21   | 4.19   | 5.47  | 3.26  | 4.34   | 4.06   | 6.11   | 0.43   | 10.31 | 26.52 | 13.72 |
| Ni   | 0.14               | 0.13  | 0.13  | 0.13  | -     | 0.18  | 0.02  | 0.10   | 0.32   | 0.04   | 0.36  | -     | 0.02   | 0.33   | -      | 0.27   | 0.13  | 0.08  | 0.13  |
| As   | 0.09               | 0.27  | 0.24  | 0.26  | 0.53  | 0.10  | 0.16  | 0.29   | 0.28   | -      | -     | 0.48  | 0.22   | 0.24   | -      | 0.40   | 0.40  | 0.44  | 0.41  |
| S    | 0.17               | 0.28  | 0.06  | 0.06  | 0.02  | 0.18  | -     | 0.21   | 0.87   | 0.36   | 0.30  | 0.10  | 0.12   | -      | 0.05   | 0.17   | 0.17  | 0.04  | 0.15  |

Analysis 2G1B corresponds to the Pt<sub>3</sub>Cu term (coexisting with Pt<sub>3</sub>Fe, analysis 2G1A) and analysis 2G1C corresponds to the recalculated composition of the initial grain 2G1; - = not detected.

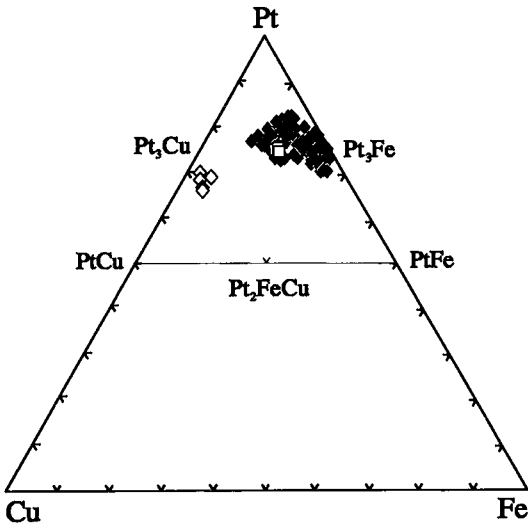


FIG. 5. Plot of compositions of Pt-Fe alloys (atom %) in the Pt-Fe-Cu diagram. Open symbols correspond to  $Pt_3Cu$  and  $Pt_3Fe$  phases of nugget 2G1.

tion involves substitution for Pt. The maximum content of Ir+Ru+Os reaches 10 at.%, and the range in isoferroplatinum is (in wt.%): 0 to 2.6 for Os, 0 to 5.9 for Ir, and 0 to 3.4 for Ru. The low content of Os is probably due to its relative low solubility in  $Pt_3Fe$  owing to crystallochemical constraints. Note also the broad positive

correlation between Rh and Ru (Fig. 9), and between Rh and Ir (Fig. 10), whereas Ru and Ir are not correlated. Os, Ir and Ru do not enter the structure of isoferroplatinum having a high Pd content, which confirms the predominant role of Pd in the substitution of Pt for other PGE. Other elements, such as Ni and As, also have been detected in isoferroplatinum. The concentration of Ni, generally close to 0.05 wt.%, may reach 0.1 wt.%, whereas that of As is more variable, with a maximum of 0.5 wt.%.

Au was detected in only one nugget (1A4). Values obtained for Au in this nugget vary between 0.5 and 1 wt.%, whereas X-ray scanning images reveal that gold also is present as minute inclusions in the nugget.

More interesting are the relationships between isoferroplatinum composition and the nature and characteristics of included phases. For example, Figure 11 illustrates the Ir content of nuggets with and without PGM inclusions. It can clearly be seen that the very low Ir values are mainly restricted to nuggets without included phases containing Ir, whereas the highest Ir values correspond to nuggets containing trapped Os-Ir alloys. Inclusion-bearing nuggets plotting in the field of inclusion-free nuggets do not contain inclusions of iridium minerals. In the same way, nugget B2, having the highest Ru content (3.4 wt.%), is also very laurite-rich; nuggets B16, 1A4, 1A5, with the highest Pd values, contain numerous included Pd-minerals, and nugget 1B3, the richest in Rh, also contains included Rh-minerals.

Hence it appears that the nature of the PGE present in solid solution in isoferroplatinum reflects the nature of

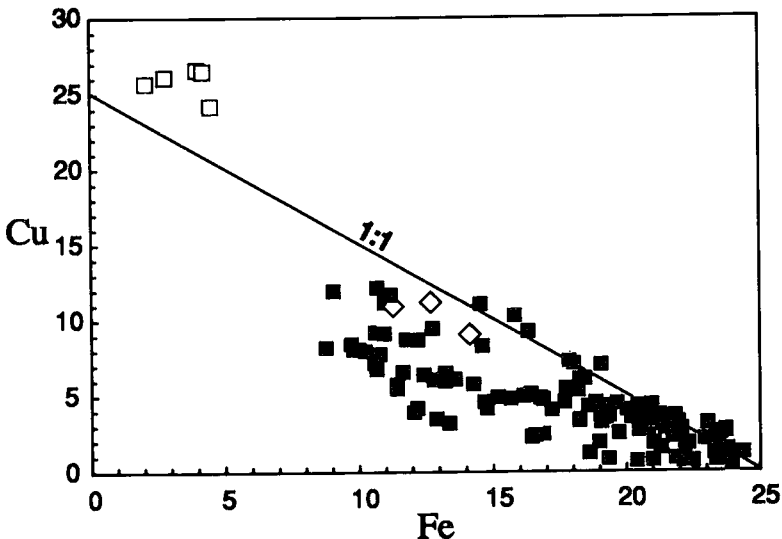


FIG. 6. Plot of Cu versus Fe (atom %) for Pt-Fe alloys. Open symbols correspond to the Cu-rich and Fe-rich compositions of nugget 2G1.

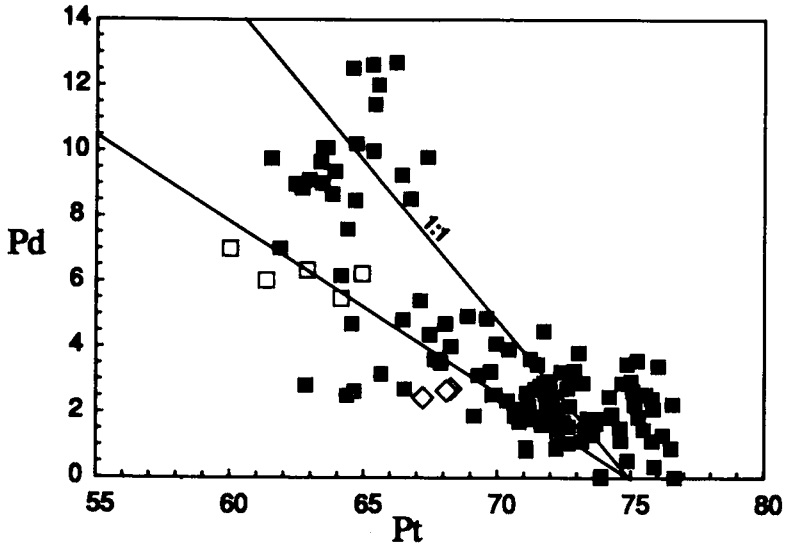


FIG. 7. Plot of Pd versus Pt (atom %) for Pt-Fe alloys, with indication of the two trends of substitution. Open symbols correspond to the Cu-rich and Fe-rich compositions of nugget 2G1.

the included PGM in the host isoferroplatinum. This observation has to be related to the composition of the medium from which the PGM crystallized; an environment rich in Pd and Rh, for example, will give isoferroplatinum with a high Rh content that will trap Rh-minerals. Similarly, a medium enriched in Ru will give

Ru-rich  $Pt_3Fe$  containing laurite trapped from the environment. However, two parameters in competition have to be envisaged: the chemical composition of the medium and the respective solubility of the different PGE in  $Pt_3Fe$ . The nature of included phases permits us to quantify the first parameter (*e.g.*, presence of laurite

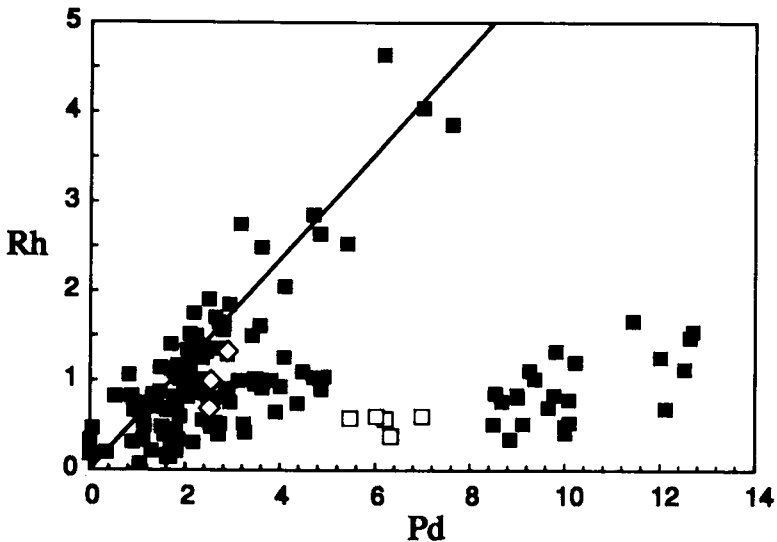


FIG. 8. Plot of Rh versus Pd (atom %) for Pt-Fe alloys. Open symbols correspond to the Cu-rich and Fe-rich compositions of nugget 2G1. Other points plotting outside the substitution line belong to nuggets B16, 1A4, and 1A5.

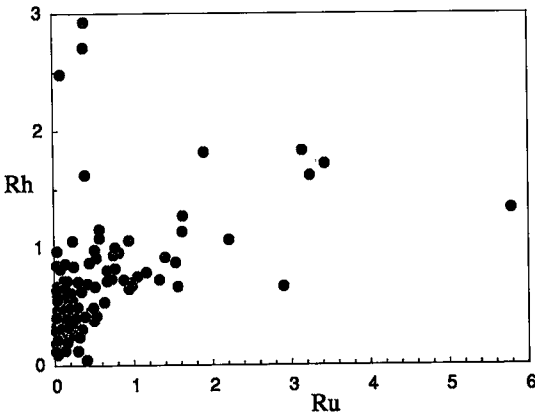


FIG. 9. Plot of Rh versus Ru (atom %) for isoferroplatinum nuggets.

inclusions implies presence of Ru in the medium), which enables us to establish empirically the relative solubility of the PGE in  $Pt_3Fe$ : (1) Pd, (2) Rh, Ir, Ru and (3) Os.

The compositions of Pt-Fe alloys from similar environments (*i.e.*, alluvial deposits) given by Toma & Murphy (1977) for different placers correspond to the range obtained here. Note that these authors have shown that the composition of the Pt-Fe alloy is relatively placer-specific. Bowles (1981) noted that the Ir content of the Pt-Fe alloy could be specific of the environment of the nuggets. Pt-Fe nuggets from the Tulameen complex (Nixon *et al.* 1990) show much larger variations in composition, from isoferroplatinum to tetraferroplatinum, with a Pt content ranging from 71.0 to 90.2 wt.%. A relatively large range of composition also has

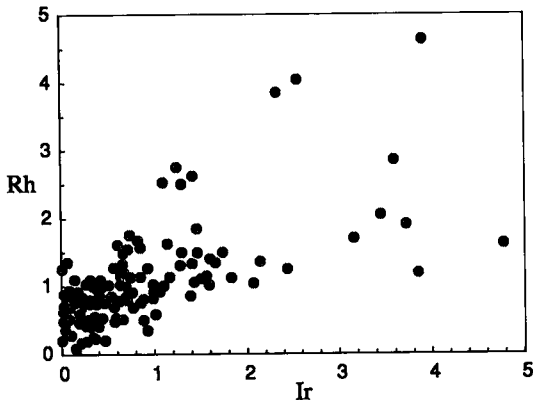


FIG. 10. Plot of Rh versus Ir (atom %) for isoferroplatinum nuggets.

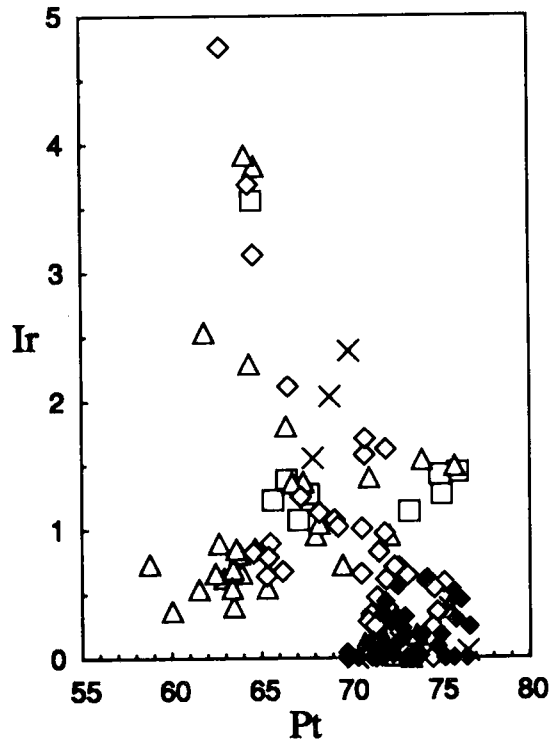


FIG. 11. Plot of Ir versus Pt (atom %) for isoferroplatinum nuggets: Symbols are a function of the nature of the included PGM in the nuggets: open diamond: Os-rich alloy (inclusion and exsolution), cross: laurite, square: laurite and alloys, triangle: complex assemblages, closed diamond: nuggets without inclusion.

been obtained by Johan *et al.* (1990) for Pt-Fe alloy from the Durance River alluvium, but contrary to the observations made here, a correlation between iron and other elements was not observed. Slansky *et al.* (1991) gave compositions of isoferroplatinum from the Fifield area (Australia), and reported variable amounts of PGE.

#### $Pt_3Cu$

Platinum nugget 2G1 is composed of  $Pt_3Fe$  and a  $Pt_3Cu$  phase (Table 1). Textural relationships suggest an origin by unmixing (Fig. 2C). The proportion of the Cu-rich phase has been estimated using image analysis at 20% of the whole nugget. This estimate enables us to calculate the original composition of the nugget (Table 2), close to  $Pt_3FeCu$ . At about 650°C (Hansen & Anderko 1958), the  $Pt_3Cu$  composition is not stable, and  $Pt_3Cu$  and  $Pt_3Cu_7$  coexist instead to low temperature. Therefore, in the Pt-Fe-Cu system, the nugget analyzed here indicates unmixing to give two contrasted compo-

sitions (close to  $Pt_6Pd_{0.7}Cu_{2.7}Fe_{0.4}$  and  $Pt_7Pd_{0.2}Cu_1Fe_{1.6}$ , respectively). Thus one may consider that the initial  $Pt_3(Cu_{0.5}Fe_{0.5})$  compound will give two phases, with a composition close to  $Pt_3Fe$  and  $Pt_3Cu$ , respectively.

The  $Pt_3Fe$  phase of this nugget cannot be distinguished from isoferroplatinum of other nuggets; its Cu content, approximately 10–12 at.%, is high, but in the range of other nuggets (Figs. 5, 6), whereas its Pd content is low (3 at.%, Figs. 7, 8), which implies a low proportion of other PGE. The  $Pt_3Cu$  phase (Figs. 5, 6), which contains 2 to 4 at.% Fe, has a relatively low content of Pt (which does not exceed 65 at.%), a high content of Pd (6–7 at.%, Fig. 7), indicating a higher solubility of Pd in the Cu-rich phase, and a low content of the other PGE. Note, however, the presence of Au in minor amounts (around 0.3–0.5 at.%), which has not been detected in the coexisting  $Pt_3Fe$ . Analyses show a slight deficiency in PGE compared to ideal  $Pt_3Cu$ , and the formula obtained is  $(Pt_{60-65}Pd_{5-7}Other_1)_{68-72}(Cu_{24-27}Fe_{2-5})_{26-32}$ .

There is a rim about 20  $\mu m$  thick devoid of Cu-rich unmixing phase on the nugget. This rim has the same composition as the other part of the crystal. The presence of this rim indicates that the morphology of the nugget is primary and has not undergone modification after its crystallization. Also, structures appearing within the nugget are interpreted to correspond to four families of cleavages (Fig. 2C) that define the octahedron planes of a cubic structure. Cleavage has never been reported in minerals of the Pt-Fe family. Similar structures were observed by Slansky *et al.* (1991), but were interpreted as "scars" left after the removal of exsolution lamellae of Os-Ir-Ru alloy during secondary processes.

## COMPOSITION OF PGM INCLUDED IN THE PLATINUM NUGGETS

### Os-Ir-Ru alloy

An alloy of Os-Ir-Ru is the most abundant PGM found as inclusions in the isoferroplatinum nuggets. It occurs either as exsolution lamellae less than 1  $\mu m$  thick, as trapped laths (1 to 10  $\mu m$  thick), in some cases, organized as sheaves (Fig. 2E), or as larger crystals (Fig. 3B). The Os-Ir-Ru alloy also forms extremities of inclusions of iridium oxide (Figs. 4B, C, D). In one case, large grains of an Os-Ir-Ru alloy are cemented only by isoferroplatinum (*i.e.*, composite grain 1G5). The composition of the Os-Ir-Ru alloy (Table 3) is relatively homogeneous (Fig. 12) and corresponds to osmium according to Harris & Cabri (1991). The range recorded (in wt.%) is 0.1–17.4 (av. 4.6) for Ru, 1.2–34.6 (av. 14.6) for Ir, and 53.0–98.1 (av. 75.0) for Os. Within a given nugget, variations in the composition of the alloy have been observed. In laths, the compositional trend is marked by a moderate Ru-for-Os substitution. For larger grains, compositional zoning has been noted along two different trends. In the nugget B2, the alloy is characterized by a core of a pure Os composition and a Ru-rich rim, showing the Ru-for-Os substitution. The presence of a large compositional gap between rim and core is observed. The composition of the Ru-rich rim corresponds to the composition of the coexisting lath of alloy in the same nugget. In nugget B11, a large inclusion of alloy (Fig. 3B) is marked by normal and inverse zoning, *i.e.*, an Os-rich core, an intermediate part with a decrease in Os correlated with an increase in Ir, and an Os-rich

TABLE 3. SELECTED ELECTRON-MICROPROBE DATA OF PGE ALLOYS INCLUDED IN ISOFERROPLATINUM NUGGETS

|      | B2                 | B3    | 1A1    | 1A5   | 1A4    | 2G5    | B8     | 2G2   | B11   | 1A3   | B5    | B13   | 2G4    | B2     |
|------|--------------------|-------|--------|-------|--------|--------|--------|-------|-------|-------|-------|-------|--------|--------|
|      | Weight per cent    |       |        |       |        |        |        |       |       |       |       |       |        |        |
| Os   | 61.66              | 67.02 | 68.33  | 71.83 | 73.79  | 74.88  | 77.26  | 78.74 | 81.92 | 84.44 | 84.54 | 84.95 | 94.11  | 96.31  |
| Ir   | 14.08              | 20.97 | 18.49  | 11.12 | 16.45  | 20.87  | 13.29  | 16.99 | 13.40 | 5.70  | 9.81  | 10.29 | 1.37   | 3.13   |
| Ru   | 15.32              | 3.28  | 5.70   | 8.25  | 4.68   | 2.48   | 3.75   | 0.41  | 0.49  | 3.76  | 1.01  | 0.50  | 0.52   | 0.50   |
| Pt   | 7.53               | 6.95  | 6.06   | 5.93  | 3.83   | 2.05   | 4.78   | 2.79  | 3.25  | 5.13  | 3.66  | 3.34  | 4.13   | 1.27   |
| Pd   | 0.05               | -     | -      | -     | -      | -      | 0.16   | 0.01  | -     | 0.27  | -     | 0.19  | 0.42   | 0.03   |
| Rh   | 1.02               | 0.77  | 0.34   | 0.65  | 0.31   | 0.15   | 0.55   | 0.45  | 0.05  | 0.14  | 0.45  | 0.10  | 0.02   | 0.05   |
| Fe   | 0.25               | 0.36  | 0.55   | -     | 0.77   | -      | 0.33   | -     | 0.13  | -     | 0.02  | -     | 0.04   | -      |
| Ni   | 0.01               | 0.15  | 0.02   | 0.03  | -      | 0.03   | -      | -     | 0.03  | 0.02  | 0.01  | 0.06  | -      | 0.04   |
| Cu   | 0.14               | 0.13  | 0.35   | 0.28  | 0.17   | 0.14   | 0.18   | 0.18  | 0.16  | 0.08  | 0.09  | 0.10  | -      | 0.02   |
| As   | 0.21               | -     | 0.21   | 0.17  | 0.27   | 0.06   | 0.00   | 0.31  | 0.18  | 0.07  | 0.28  | -     | 0.29   | 0.01   |
| S    | -                  | 0.01  | -      | -     | -      | 0.04   | 0.05   | -     | 0.04  | -     | -     | 0.04  | -      | 0.02   |
| Tot. | 100.26             | 99.63 | 100.05 | 98.25 | 100.25 | 100.70 | 100.33 | 99.88 | 99.66 | 99.61 | 99.88 | 99.57 | 100.88 | 101.37 |
|      | Atomic proportions |       |        |       |        |        |        |       |       |       |       |       |        |        |
| Os   | 53.37              | 64.29 | 63.62  | 67.32 | 68.99  | 72.44  | 73.33  | 77.79 | 81.03 | 81.67 | 83.15 | 84.46 | 92.17  | 94.41  |
| Ir   | 12.05              | 19.90 | 17.03  | 10.31 | 15.22  | 19.98  | 12.48  | 16.61 | 13.11 | 5.45  | 9.55  | 10.12 | 1.32   | 3.04   |
| Ru   | 24.96              | 5.92  | 9.98   | 14.55 | 8.23   | 4.52   | 6.69   | 0.75  | 0.92  | 6.84  | 1.88  | 0.94  | 0.95   | 0.92   |
| Pt   | 6.36               | 6.50  | 5.50   | 5.42  | 3.49   | 1.93   | 4.42   | 2.69  | 3.13  | 4.84  | 3.51  | 3.24  | 3.94   | 1.21   |
| Pd   | 0.07               | -     | -      | -     | -      | -      | 0.27   | 0.02  | -     | 0.46  | -     | 0.34  | 0.73   | 0.05   |
| Rh   | 1.63               | 1.37  | 0.59   | 1.12  | 0.53   | 0.26   | 0.96   | 0.83  | 0.10  | 0.25  | 0.81  | 0.19  | 0.03   | 0.10   |
| Fe   | 0.73               | 1.18  | 1.75   | -     | 2.44   | -      | 1.05   | -     | 0.44  | -     | 0.08  | -     | 0.12   | -      |
| Ni   | 0.02               | 0.46  | 0.06   | 0.09  | -      | 0.10   | -      | -     | 0.10  | 0.08  | 0.04  | 0.19  | -      | 0.11   |
| Cu   | 0.35               | 0.36  | 0.98   | 0.79  | 0.46   | 0.41   | 0.52   | 0.53  | 0.46  | 0.23  | 0.28  | 0.31  | -      | 0.05   |
| As   | 0.46               | -     | 0.48   | 0.40  | 0.64   | 0.15   | 0.00   | 0.78  | 0.46  | 0.18  | 0.70  | -     | 0.73   | 0.02   |
| S    | -                  | 0.02  | -      | -     | -      | 0.21   | 0.28   | -     | 0.25  | -     | -     | 0.22  | -      | 0.09   |

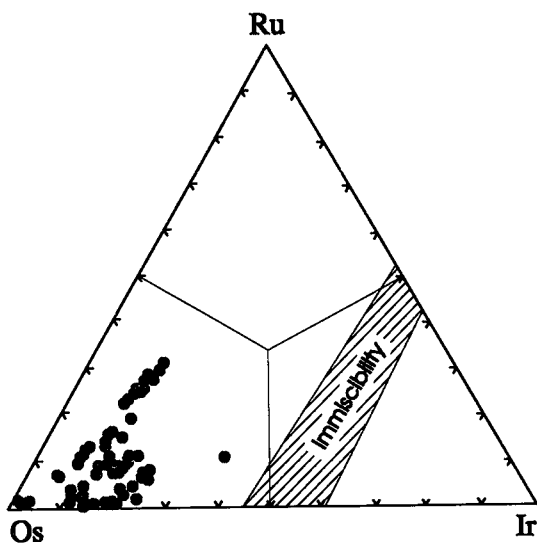


FIG. 12. Plot of compositions of osmium inclusions (atom %) in the Os-Ir-Ru diagram.

rim. The general trend here is Ir-for-Os substitution. Törnroos & Vuorelainen (1987) reported two trends from core to rim: one with (Ir+Ru)-for-Os substitution, and one with Ir-for-Os substitution.

In some cases, the Pt content of the osmium minerals can be attributed to the surrounding isoferroplatinum, also intersected by the electron beam. However, the presence of Pt in the structure of the alloy is confirmed by the larger inclusions (where it may reach 6 wt.%) and by the osmium from the complex nuggets, where it reaches 2 wt.%. Owing to their crystallographic similarities, Pt is likely to substitute for Ir in the structure. This is confirmed by Slansky *et al.* (1991), who described Pt-bearing iridium alloys (with up to 15 wt.% Pt) coexisting with osmium alloy, with a maximum of 3 wt.% Pt.

Other minor elements encountered in the osmium inclusions (Table 3) are As (0 to 0.4 wt.%), Cu (0 to 0.6 wt.%), Pd (generally lower than the detection limit, but up to 0.4 wt.% in some minerals), and Rh (systematically present, from 0.1 to 1.0 wt.%). In contrast, Ni and S are almost always below the detection limit.

The presence of laths and exsolution lamellae of Os-Ir alloy in Pt-Fe nuggets has been described by many investigators (Cousins & Kinloch 1976, Feather 1976, Toma & Murphy, 1977, Cabri *et al.* 1981, Bowles 1981, Törnroos & Vuorelainen 1987, Johan *et al.* 1991, Slansky *et al.* 1991). Compositions given by Toma & Murphy (1977) show a much higher Ir content than that recorded here (reaching 80 wt.%, *i.e.*, iridium). Large variations in the composition of alloys were reported by Törnroos & Vuorelainen (1987) (with a relative enrichment in Ru), and by Johan *et al.* (1991). Os-rich compositions, similar to those obtained here, are given

by Bowles (1981) for nuggets from Sierra Leone and by Cabri *et al.* (1981) for nuggets from Ethiopia. Johan *et al.* (1990) discovered only one inclusion of Os alloy in isoferroplatinum, consisting of almost pure Os. Thus, the Ir/Os ratio of the included alloys might be specific of the geological environment of the source.

Os-Ir-Ru alloy is commonly found in placers as a discrete phase (Harris & Cabri 1973, Cabri & Harris 1975). Compared to the composition of the alloy included in isoferroplatinum, the alloy forming a discrete mineral in placers is enriched in Ir and Ru and shows much larger compositional variations. Similarly, the alloy included in ophiolitic chromitites (Legendre & Augé 1986, Augé & Johan 1988) is characterized by a large range in composition.

#### *Laurite - erlichmanite series*

Ru sulfide (laurite) and Os sulfide (erlichmanite) occur as trapped crystals within isoferroplatinum nuggets or in the composite nugget 2G5. Where included, their size can reach 50  $\mu\text{m}$ . They occur either as euhedral or roundish crystals. Their relationships with the host crystal are complex; they have been observed as: 1) small euhedral crystals at the periphery of the nugget (Fig. 2D); this suggests trapping of laurite during the final stage of the growth of the isoferroplatinum and absence of evolution of the nugget after this trapping, 2) abundant small crystals randomly disposed in the host; their entrapment follows the rapid nucleation of laurite (both suggesting growth from a S-rich medium), 3) crystals included in (or adjacent to) other sulfides, which are themselves included in the nuggets [*i.e.*, cooperite (Fig. 3A) or braggite (Fig. 4A)], 4) large individual grains included in isoferroplatinum.

Representative compositions of laurite and erlichmanite are given in Table 4. A plot of sulfide compositions in the ternary system covers the whole Ru-Os compositional range, at a low Ir content (Fig. 13).

In some nuggets, two generations of Ru-Os sulfide have been distinguished: large crystals close to  $\text{RuS}_2$ , and smaller zoned crystals. These zoned crystals are either laurite or erlichmanite, each with a rim enriched in Os (nugget B11, Fig. 2F). Note that the zoned crystal of laurite coexists in this nugget with zoned Os-Ir alloy. Textural features do not permit the determination of relationships between the two types of sulfides, but previous work (Legendre 1982, 1990) has shown that the Ru-rich phase is earlier than the Os-rich one, assuming an increase of the  $f(\text{S}_2)$  during crystallization. In the whole sequence of crystallization, Os-Ir-Ru alloy has crystallized prior to Ru-rich sulfide. The abundant small crystals of Os-rich laurite disseminated in nugget B6 are postulated to have crystallized during a rise in  $f(\text{S}_2)$ .

Minor elements encountered in the laurite-erlichmanite series (Table 4) consist of As (from 0 to 0.5 wt.%), Fe (0 to 0.7 wt.%), Pd [0 to 0.4 wt.%, but up to

TABLE 4. SELECTED ELECTRON-MICROPROBE DATA OF PGE SULFIDES AND SULFARSENIDES INCLUDED IN ISOFERROPLATINUM NUGGETS

|      | Laurite-Erichmanite |        |       |       |        |       |       |       | Cooperite |       |        |       | Braggite |        | Kashinite |       |     | Holl. |
|------|---------------------|--------|-------|-------|--------|-------|-------|-------|-----------|-------|--------|-------|----------|--------|-----------|-------|-----|-------|
|      | 2G5                 | B3     | B11   | B16   | B2     | B10   | 2G3   | B6    | 2G5       | B10   | B10    | B16   | B16      | B16    | B16       | 1B3   | B16 |       |
|      | Weight per cent     |        |       |       |        |       |       |       |           |       |        |       |          |        |           |       |     |       |
| Os   | 0.20                | 2.67   | 3.63  | 4.80  | 5.77   | 24.87 | 25.79 | 26.36 | 48.51     | -     | -      | -     | -        | -      | -         | -     | -   | 0.70  |
| Ir   | -                   | 1.60   | 1.09  | 2.24  | 1.58   | 1.06  | 3.89  | 0.85  | 6.65      | -     | -      | -     | 0.81     | 10.85  | 36.99     | 26.79 | -   | 27.98 |
| Ru   | 56.77               | 54.49  | 54.48 | 46.60 | 51.81  | 34.81 | 32.87 | 29.71 | 14.11     | -     | -      | 0.15  | 0.15     | -      | 0.02      | -     | -   | 1.16  |
| Pt   | 1.90                | 1.00   | 0.31  | 2.39  | 1.96   | 2.73  | 1.05  | 5.11  | 0.63      | 81.87 | 81.92  | 74.49 | 52.31    | 1.79   | 3.61      | 5.61  | -   | 2.72  |
| Pd   | 0.27                | -      | -     | 3.77  | -      | -     | -     | 0.17  | 0.41      | 2.87  | 3.28   | 8.70  | 28.22    | 6.79   | 0.13      | 0.16  | -   | 0.61  |
| Rh   | 1.33                | 1.99   | 1.34  | 4.06  | 2.07   | 2.26  | 1.76  | 3.04  | 0.55      | 0.19  | 0.45   | 0.51  | -        | 51.35  | 31.22     | 38.11 | -   | 24.47 |
| Fe   | 0.40                | -      | -     | -     | -      | -     | -     | 0.17  | 0.13      | -     | -      | -     | 0.10     | 0.06   | 0.21      | 0.79  | -   | 0.03  |
| Ni   | -                   | -      | 0.07  | -     | 0.03   | 0.02  | 0.05  | 0.04  | -         | 0.08  | 0.09   | 0.09  | 0.11     | 0.01   | 0.02      | -     | -   | -     |
| Cu   | -                   | -      | -     | 0.06  | 0.14   | 0.10  | 0.03  | 0.07  | 0.09      | -     | -      | 0.08  | 0.22     | 0.70   | 0.55      | 0.52  | -   | 0.34  |
| As   | -                   | 0.20   | 0.05  | 0.00  | 0.17   | 0.23  | 0.04  | 0.26  | 0.07      | 0.13  | 0.02   | 0.26  | 0.05     | 0.03   | -         | 0.16  | -   | 26.44 |
| S    | 39.17               | 38.48  | 38.75 | 35.78 | 38.56  | 33.77 | 33.85 | 32.72 | 27.79     | 14.05 | 14.67  | 14.72 | 18.38    | 29.80  | 25.29     | 27.28 | -   | 13.89 |
| Tot. | 100.04              | 100.42 | 99.71 | 99.69 | 102.08 | 99.85 | 99.33 | 98.48 | 98.94     | 99.17 | 100.43 | 99.00 | 100.35   | 101.63 | 98.02     | 99.42 | -   | 98.34 |
|      | Atomic proportions  |        |       |       |        |       |       |       |           |       |        |       |          |        |           |       |     |       |
| Os   | 0.06                | 0.78   | 1.07  | 1.48  | 1.70   | 8.30  | 8.68  | 9.10  | 19.42     | -     | -      | -     | -        | -      | -         | -     | -   | 0.30  |
| Ir   | -                   | 0.47   | 0.32  | 0.68  | 0.46   | 0.35  | 1.30  | 0.29  | 2.63      | -     | -      | -     | 0.38     | 3.59   | 14.61     | 9.85  | -   | 12.03 |
| Ru   | 30.92               | 30.14  | 30.13 | 27.09 | 28.66  | 21.87 | 20.83 | 19.30 | 10.63     | -     | -      | 0.16  | 0.14     | -      | 0.02      | -     | -   | 0.95  |
| Pt   | 0.54                | 0.29   | 0.09  | 0.72  | 0.56   | 0.89  | 0.35  | 1.72  | 0.25      | 47.17 | 45.92  | 40.81 | 23.94    | 0.58   | 1.40      | 2.03  | -   | 1.15  |
| Pd   | 0.14                | -      | -     | 2.08  | -      | -     | -     | 0.10  | 0.30      | 3.03  | 3.37   | 8.74  | 23.68    | 4.06   | 0.09      | 0.11  | -   | 0.48  |
| Rh   | 0.71                | 1.08   | 0.73  | 2.32  | 1.12   | 1.40  | 1.10  | 1.94  | 0.41      | 0.20  | 0.48   | 0.53  | -        | 31.78  | 23.03     | 26.16 | -   | 19.65 |
| Fe   | 0.39                | -      | -     | -     | -      | -     | -     | 0.20  | 0.18      | -     | -      | -     | 0.16     | 0.06   | 0.28      | 1.00  | -   | 0.04  |
| Ni   | -                   | -      | 0.06  | -     | 0.02   | 0.03  | 0.05  | 0.04  | -         | 0.15  | 0.16   | 0.17  | 0.16     | 0.01   | 0.02      | -     | -   | -     |
| Cu   | -                   | -      | -     | 0.06  | 0.12   | 0.10  | 0.03  | 0.07  | 0.11      | -     | -      | 0.13  | 0.31     | 0.70   | 0.66      | 0.58  | -   | 0.44  |
| As   | -                   | 0.15   | 0.04  | 0.00  | 0.12   | 0.20  | 0.04  | 0.23  | 0.07      | 0.19  | 0.03   | 0.37  | 0.06     | 0.02   | -         | 0.15  | -   | 29.16 |
| S    | 67.25               | 67.10  | 67.57 | 65.57 | 67.23  | 66.88 | 67.63 | 67.01 | 66.01     | 49.25 | 50.04  | 49.09 | 51.18    | 59.18  | 59.90     | 60.11 | -   | 35.80 |

4.6 wt.% in laurite adjacent to a braggite crystal (Fig. 4A)] and Rh (at a rather high value, between 0.6 and 4 wt.%, and up to 8.8 wt.% in one grain of laurite, in a clear case of Rh-for-Ru substitution). Slansky *et al.* (1991) considered a high Rh content in laurite to be typical of Alaskan-type and layered intrusions.

Except in tiny crystals, where a positive Pt-Fe correlation indicates contamination due to the impingement of the electron beam on the host crystal, Pt enters into the structure of the sulfide in significant amounts. The Pt content in the laurite not included in isoferroplatinum of the composite nugget 2G5 is 1.9 wt.%, whereas it ranges from 0.3 to 3.8 in larger grains included in isoferroplatinum. Note that this Pt enrichment seems to be characteristic of laurite crystallizing from a medium rich in Pt. For example, laurite in ophiolitic chromitite (Legendre & Augé 1986, Augé 1988) is totally devoid of Pt. Thus the Pt content of laurite could be used as an indicator of the Pt content of the medium from which it formed.

Laurite and erlichmanite inclusions have been described in nuggets from different placers (Cousins & Kinloch 1976, Toma & Murphy 1977, Bowles 1981, Cabri *et al.* 1981, Slansky *et al.* 1991), whereas Johan *et al.* (1990) stressed the absence of laurite in nuggets from the Durance River. Therefore, the occurrence of Os-Ru sulfide inclusions could be specific of the environment.

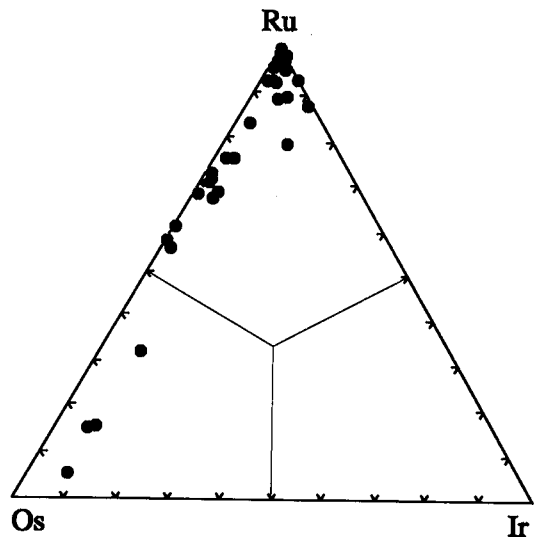


FIG. 13. Plot of compositions of laurite and erlichmanite (atom %) in the Ru-Os-Ir diagram.

### Cooperite – braggite

Four crystals of braggite have been found in isoferroplatinum nugget B16, two of cooperite in nugget B10, and one in nugget B4. Braggite occurs either as euhedral inclusions associated with other PGM (mainly laurite, Fig. 4A), whereas cooperite forms round crystals, in some cases associated with laurite (Fig. 3A). Large variations in braggite composition have been recorded, with a Pd content ranging from 9 to 26 at.%. The composition of cooperite (Table 4) is more restricted, with a Pt content varying between 42 and 47 at.%. In both cases, Ni content is extremely low and does not exceed 0.4 at.%. This relative lack of Ni is a characteristic of these Pt–Pd sulfides, since published data invariably indicate the presence of Ni in these phases, generally around 15 at.% for braggite (Cabri *et al.* 1978, Criddle & Stanley 1985, Tarkian 1987); thus, this locality seems to provide one of the first natural occurrences of Ni-free braggite, which confirms the general Ni impoverishment observed in the nuggets. Minor elements systematically encountered in these sulfides include As (0.1 to 1.3 wt.%), Rh (0.1 to 1.4 wt.%), and Cu (0 to 0.3 wt.%).

### Kashinite

Two euhedral crystals of kashinite, (Ir,Rh)<sub>2</sub>S<sub>3</sub>, have been found in different nuggets. One is attached to an assemblage of braggite and laurite (Fig. 4A), the other is at the periphery of the host isoferroplatinum. A SEM back-scattered electron image of the former shows zoning due to oscillatory distribution of Rh and Ir, with Ir ranging from 11 to 37 wt%, and Rh ranging from 31 to 51 wt% (Table 4, nugget B16). Note that significant levels of Pd (*i.e.*, 6.8 wt%) accompany the Rh-rich phase, whereas Pt is found in the Ir-rich phase (3.6 wt%). The second crystal shows an intermediate composition, although it is richer in Pt. Other elemental abundances are not significant, except copper, which ranges from 0.4 to 0.7 wt%.

The first occurrence of kashinite (Begizov *et al.* 1985) was described in a similar context, as inclusions in isoferroplatinum nuggets in placer from the Ural Mountains. It occurs either isolated or attached to other complex sulfides. Slansky *et al.* (1991) have also described minerals of the kashinite–bowieite series included in isoferroplatinum nuggets from the Fifield Complex.

### Hollingworthite

Two crystals of hollingworthite (RhAsS) have been found, both adjacent to laurite. One crystal is too small to be analyzed, but the second appears heterogeneous, marked by Ir-for-Rh substitution. Compositions given in Table 4 are from the Ir-rich zone. Note that the associated laurite (nugget B16) also is enriched in Ir.

Cabri *et al.* (1981) mentioned the presence of “numerous, discrete blebs of hollingworthite, up to 5 µm in size” in one nugget from Ethiopia.

### Keithconnite

Nine crystals of keithconnite (Pd<sub>3-x</sub>Te) have been found in four nuggets. Keithconnite occurs either as: isolated crystals attached to the surface of the nugget (1A4), isolated crystals adjacent to a lath of osmium within nugget (1A5), and minute crystals found within a complex assemblage. In this case, keithconnite coexists with Pd–Pt–Cu–S minerals (B16, 2G3, Figs. 3C, D, E).

Crystal size varies between 2 and 25 µm. The composition of all the crystals (Table 5) is homogeneous, whatever the context, and is close to the formula Pd<sub>3</sub>Te, with a weak deficiency in Pd. Minor elements present consist of Pt (1 to 3 wt.%), As (0 to 0.7 wt.%), and Cu (0 to 0.2 wt.%). Such elements are compatible with values recorded in the Stillwater Complex by Cabri *et al.* (1979). Note that the stability of Pd<sub>3</sub>Te is not confirmed by recent experimental work carried out at atmospheric pressure below 1000°C (Kim *et al.* 1990).

### Unnamed minerals

All the minerals described in this section are inclusions either comprising rounded polymineralic inclusions (described as globules) or euhedral composite assemblages. Their size is generally small, less than one µm, up to a few µm. For the former, only qualitative analyses have been obtained. They essentially consist of (Pt,Pd,Rh,Cu,Ni) sulfides, and only one alloy (containing Pt, Pd, Au and Cu) has been found.

Compositions are presented in Table 5 and suggest the following formulae (numbers correspond to those given in Table 5): 1) (Pd,Pt)<sub>3</sub>(Te,As), 2) Pd<sub>4</sub>S, 3) (Pd,Pt)<sub>2</sub>S, 4) (Pd,Pt)<sub>3</sub>(Cu,Ni)S<sub>2</sub>, 5) Cu(Rh,Pt)<sub>2</sub>S<sub>4</sub>, 6) (Pd,Pt)<sub>2</sub>(Rh,Ir)(Cu,Ni)S<sub>4</sub>, 7) (Pd,Pt,Au)<sub>2</sub>Cu, and 8) (Pt,Pd,Rh,Os,Au,Cu)<sub>3</sub>S<sub>2</sub>.

Mineral 1 (see above and Table 5) can be compared to vincentite (Stumpfl & Tarkian 1974), originally described from a similar context. Our compositions differ from the published composition only by the absence of Sb, which is compensated by a higher Te content. Mineral 5 can be considered as a cuprorhodsite with the formula (Cu<sub>0.9</sub>Ni<sub>0.1</sub>)(Rh<sub>1.1</sub>Pt<sub>0.7</sub>Pd<sub>0.2</sub>)S<sub>4</sub>. Similar compositions were given by Johan *et al.* (1990) for minerals associated with bornite, included in nuggets, and interpreted as exsolution from a complex Pt–Rh–Cu–Fe solid solution enriched in S.

The above minerals form globular inclusions composed of several phases. Only two nuggets contain these inclusions: B16 and 2G3. In addition, nugget B16 contains assemblages of euhedral inclusions, where globular and euhedral inclusions are preferentially dis-

TABLE 5. ELECTRON-MICROPROBE DATA OF VARIOUS PGM INCLUDED IN ISOFERROPLATINUM NUGGETS

|      | Keithconnite       |        |        | 1     | 2      |        | 3      |        | 4     |       | 5      |       | 6     |      | 7      |       | 8   |  | Ir Oxide |  |
|------|--------------------|--------|--------|-------|--------|--------|--------|--------|-------|-------|--------|-------|-------|------|--------|-------|-----|--|----------|--|
|      | B16                | B16    | 1A5    | B16   | B16    | B16    | B16    | B16    | 2G3   | 2G3   | 2G3    | 2G3   | 2G3   | 2G3  | 2G3    | 2G3   | B13 |  |          |  |
|      | Weight per cent    |        |        |       |        |        |        |        |       |       |        |       |       |      |        |       |     |  |          |  |
| Pt   | 2.81               | 1.88   | 0.84   | 12.79 | 2.81   | 2.05   | 4.44   | 5.01   | 11.17 | 28.77 | 26.44  | 24.09 | 36.13 | Ir   | 69.27  | 62.57 |     |  |          |  |
| Pd   | 70.53              | 70.40  | 70.32  | 63.85 | 87.93  | 91.28  | 79.49  | 80.67  | 58.64 | 6.18  | 20.10  | 46.00 | 14.69 | Ru   | 2.19   | 3.07  |     |  |          |  |
| Rh   | -                  | -      | -      | -     | 0.48   | -      | -      | -      | 2.87  | 23.13 | 18.44  | -     | 7.57  | Os   | -      | -     |     |  |          |  |
| Ir   | -                  | -      | -      | 0.31  | -      | -      | 0.03   | -      | -     | 2.42  | 3.37   | -     | 1.91  | Pt   | 14.76  | 13.40 |     |  |          |  |
| Os   | -                  | -      | 0.26   | 0.79  | 0.15   | -      | -      | -      | -     | -     | -      | -     | 5.00  | Pd   | -      | 0.24  |     |  |          |  |
| Ru   | -                  | -      | -      | -     | -      | -      | -      | -      | -     | -     | -      | -     | -     | Rh   | 0.40   | 0.21  |     |  |          |  |
| Au   | -                  | -      | 0.54   | -     | -      | -      | -      | -      | -     | -     | -      | -     | 6.36  | Fe   | 0.96   | 3.85  |     |  |          |  |
| Fe   | 0.19               | -      | 0.14   | 1.25  | 0.15   | 0.19   | 0.39   | 0.01   | -     | -     | 0.79   | -     | -     | Cu   | 0.78   | 0.67  |     |  |          |  |
| Cu   | 0.06               | 0.10   | 0.13   | 0.60  | 3.52   | 0.75   | 4.51   | 4.04   | 10.47 | 10.80 | 8.81   | 20.84 | 10.65 | Ni   | -      | -     |     |  |          |  |
| Ni   | 0.08               | 0.05   | 0.04   | -     | 0.02   | 0.07   | 0.08   | 0.07   | 0.22  | 1.26  | 1.77   | 0.07  | 0.40  | S    | -      | 0.08  |     |  |          |  |
| S    | -                  | 0.01   | -      | 0.46  | 7.04   | 7.18   | 11.88  | 11.71  | 13.07 | 26.39 | 21.85  | -     | 12.43 | As   | 0.09   | -     |     |  |          |  |
| As   | 0.71               | -      | 0.32   | 5.58  | 0.30   | 0.01   | 0.12   | -      | -     | -     | 0.01   | -     | -     | Tot. | 88.45  | 84.09 |     |  |          |  |
| Te   | 26.39              | 28.44  | 27.91  | 13.74 | 0.87   | 0.07   | 0.83   | 0.07   | -     | -     | 0.30   | 1.32  | 1.34  |      |        |       |     |  |          |  |
| Tot. | 100.76             | 100.88 | 100.49 | 99.36 | 103.26 | 101.61 | 101.75 | 101.57 | 96.44 | 98.95 | 101.88 | 98.68 | 92.53 |      |        |       |     |  |          |  |
|      | Atomic proportions |        |        |       |        |        |        |        |       |       |        |       |       |      |        |       |     |  |          |  |
| Pt   | 0.64               | 0.43   | 0.19   | 7.29  | 1.26   | 0.94   | 1.85   | 2.11   | 4.72  | 10.12 | 9.80   | 13.31 | 18.19 | IrO2 | 80.80  | 72.99 |     |  |          |  |
| Pd   | 29.49              | 29.51  | 29.46  | 66.71 | 72.87  | 77.31  | 60.86  | 62.42  | 45.46 | 3.99  | 13.66  | 46.61 | 13.56 | RuO2 | 2.88   | 4.04  |     |  |          |  |
| Rh   | -                  | -      | -      | -     | 0.40   | -      | -      | -      | 2.30  | 15.42 | 12.96  | -     | 7.23  | OsO2 | -      | -     |     |  |          |  |
| Ir   | -                  | -      | -      | 0.18  | -      | -      | 0.01   | -      | -     | 0.86  | 1.27   | -     | 0.98  | PtO2 | 17.18  | 15.60 |     |  |          |  |
| Os   | -                  | -      | 0.06   | 0.46  | -      | -      | -      | -      | -     | -     | -      | -     | 2.58  | PdO  | -      | 0.28  |     |  |          |  |
| Ru   | -                  | -      | -      | -     | -      | -      | -      | -      | -     | -     | -      | -     | -     | RhO2 | 0.52   | 0.28  |     |  |          |  |
| Au   | -                  | -      | 0.12   | -     | -      | -      | -      | -      | -     | -     | -      | 3.48  | 1.20  | FeO  | 1.24   | 4.95  |     |  |          |  |
| Fe   | 0.15               | -      | 0.11   | 2.48  | 0.24   | 0.32   | 0.57   | 0.01   | -     | -     | 0.45   | -     | -     | Cu2O | 0.88   | 0.75  |     |  |          |  |
| Cu   | 0.04               | 0.07   | 0.09   | 1.05  | 4.88   | 1.08   | 5.77   | 5.24   | 13.59 | 11.66 | 10.02  | 35.36 | 16.46 | NiO  | -      | -     |     |  |          |  |
| Ni   | 0.06               | 0.03   | 0.03   | -     | 0.04   | 0.10   | 0.10   | 0.10   | 0.31  | 1.47  | 2.18   | 0.13  | 0.67  | SO2  | -      | 0.16  |     |  |          |  |
| S    | -                  | 0.01   | -      | 1.58  | 19.37  | 20.17  | 30.17  | 30.08  | 33.62 | 56.48 | 49.27  | -     | 38.09 | AsO2 | 0.13   | -     |     |  |          |  |
| As   | 0.42               | -      | 0.19   | 8.27  | 0.34   | 0.02   | 0.13   | -      | -     | -     | 0.01   | -     | -     | Tot. | 103.63 | 99.04 |     |  |          |  |
| Te   | 9.20               | 9.94   | 9.75   | 11.97 | 0.60   | 0.06   | 0.53   | 0.05   | -     | -     | 0.39   | 1.12  | 1.03  |      |        |       |     |  |          |  |

posed at the periphery of the nugget. In nugget 2G3, three globules have been studied in detail; they appear more complicated than that found in the nugget B16 and are described below.

In globule 1 (Fig. 3D), four minerals have been found. The following order of crystallization is proposed: 1) keithconnite, 2) Rh-bearing malanite, 3) (Pt,Pd,Rh,Os,Au,Cu)<sub>3</sub>S<sub>2</sub> and 4) (Pd,Pt)<sub>3</sub>(Cu,Ni)S<sub>2</sub>. In globule 2 (Fig. 3E), seven minerals coexist, but only four have been determined. After the alloys (pure Os and (Pt,Pt,Au)<sub>2</sub>Cu), the order of crystallization is interpreted to be: keithconnite, followed by the complex (Pd,Pt)<sub>3</sub>(Cu,Ni)S<sub>2</sub>. The third globule contains only three phases. Figure 3F suggests the following order of crystallization: 1) crystallization of the alloy, 2) trapping of the alloy and its attached liquid droplet in the isoferroplatinum, 3) crystallization of keithconnite from the droplet, followed by an undetermined Pd,Cu sulfide. A similar situation with a lath of osmium and an attached crystal of keithconnite has already been mentioned. Note that a composition similar to (Pt,Pd)<sub>3</sub>(Cu,Ni)S<sub>3</sub> has been found in an inclusion from nugget G5, where it is associated with a large crystal of erlichmanite.

In nugget B16, five globules have been analyzed in detail. A cluster of globules (1) (Fig. 4A) disposed around the assemblage laurite-braggite-kashinite are composed of (Pt,Pd)<sub>3</sub>(Te,As), close to the ideal

stoichiometry. A similar mineralogical and textural relationship has been described by Stumpfl & Tarkian (1974). Vincentite seems associated in the inclusion with a very small crystal, which remains undetermined. Globules 2 and 3 (not shown here) both consist of keithconnite (apparently early), associated in one case with Pd<sub>4</sub>S and in the other with (Pd,Pt)<sub>2</sub>S. Pd<sub>4</sub>S also has been found in another globule (4) in association with braggite and kashinite. In globule 5 (Fig. 3C), an undetermined Pd-Cu sulfide is associated with braggite, laurite and keithconnite. Obviously, braggite is the first mineral to have crystallized. Note presence of minute particles of Os-Ir alloy preferentially associated with the sulfide (Fig. 3C).

The formulae of some of these minerals, especially minerals (2), (3), and (4) in the preceding list, show a deficit in sulfur. This feature is in good agreement with the hypothesis that the globules in which these minerals occur correspond to a trapped liquid. This liquid has then undergone fractional crystallization, as a closed system. As a result, the sulfur content of each mineral within a single globular inclusion decreases together with the succession of crystallization. This trend is especially clear from globules from the 2G3 nugget.

Many "unnamed platinum-group minerals" have been described as inclusions in Pt-Fe alloys. They occur either as euhedral minerals or as complex "blebs".

Cousins & Kinloch (1976) presented SEM images of several unnamed phases. Cabri *et al.* (1981) gave more precise compositions, Pt(Rh, Ir)CuS<sub>4</sub> and Rh(Te, Bi)<sub>2</sub>, and mentioned several unidentified Rh-Ir-Ni-Fe sulfides together with base-metal sulfide such as cubanite, chalcocopyrite and bornite. Similarly, Törnroos & Vuorelainen (1987) reported inclusions of Au-Cu-Pd alloy; Johan *et al.* (1990) reported Pt-Pd-Cu alloys and complex Pt-Pd-Cu-Rh sulfides and arsenides, and Johan *et al.* (1991) mentioned inclusions of complex Rh-Ir-Pt-Pd-Fe-Cu sulfides together with Pd-Rh arsenides and tellurides. Thus, the presence of minute inclusions dominated by Pt-Pd-Cu alloys and complex Ir-Rh-Pt-Pd-Fe-Cu sulfides is common in Pt-Fe nuggets. We suggest that the inclusions described in the literature result from the same process as that proposed here, *i.e.*, crystallization from trapped liquid droplets in a closed system.

### Iridium oxide

Inclusions in nugget B13 consist of a prismatic assemblage of crystals up to 150 × 40 μm. In general, the core region is made of a fractured iridium phase, and the extremities (and in cases, the edges) of osmium alloy. In some cases, osmium is found within the iridium phase. The ratio Os alloy:Ir phase is variable, and some inclusions appear to be composed entirely of alloy. Minute crystals of laurite may also occur at the grain boundary between Os and the host nugget (Figs. 4B, C, D).

Optical characteristics of the iridium phase (very low reflectance for a PGM), together with a low analytical total, led us to further investigate this phase. An energy-dispersion spectrometer with a light-element detector was used, and the presence of significant amount of oxygen was revealed. On the basis of the Ir content of the mineral, the formula IrO<sub>2</sub> is proposed. Calculation of the mineral's composition with the assumption that every element is present as an oxide component (Table 5), is in agreement with this hypothesis. Compared to the associated Os alloy, the Ir oxide is enriched in Pt and, to a minor extent, in Fe and Cu, but does not contain Os.

This uncommon mineral can either result from supergene alteration of an iridium alloy or by primary crystallization. An occurrence showing similarities with the one described here has been reported by Cabri *et al.* (1981), who suggested that the Ir-bearing mineral is an alteration phase containing O<sub>2</sub> and H<sub>2</sub>O; it replaces original laths of osmium. However, compositions given by Cabri *et al.* (1981) differ significantly from ours since they are much enriched in Rh, Os, and Fe for a lower Ir content and a lower analytical total than the composition obtained here.

Several features lead us to favor a primary origin for this oxide: the absence of Ir alloy in the nuggets and the elongate shape of the inclusions that does not correspond

to the habit of the cubic Ir alloy, the association with Os alloy within the lath, the size and density of the inclusion, differing from those of other nuggets, and the absence of oxidation processes in other nuggets. Thus, these assemblages are interpreted to reflect successive crystallization of iridium oxide, followed by Os alloy. This assemblage was then trapped in the isoferroplatinum nugget. The preferential presence of Os alloy at the extremities of the crystal of iridium oxide is explained by a differential growth-rate along different directions. The appearance of Os alloy within the iridium oxide (Fig. 4C) is due to recurrent growth of iridium oxide after crystallization of alloy. Note that cracks within the iridium oxide all are filled with alteration products such as kaolinite, from outside the nugget.

The composition of Os alloy associated with the oxide, with 10–13 wt.% Ir, does not differ from Os laths in other nuggets. Likewise, the laurite in this nugget plots in the compositional field defined by the other occurrences of laurite.

### COMPOSITION OF SILICATES IN THE PLATINUM NUGGETS

*Clinopyroxene* (En<sub>45.2</sub>Fs<sub>10.6</sub>Wo<sub>44.1</sub>) is characterized by relatively high Al<sub>2</sub>O<sub>3</sub>, Na<sub>2</sub>O and TiO<sub>2</sub> content (Table 6), with 0.2 wt.% Cr<sub>2</sub>O<sub>3</sub> and 0.1 wt.% NiO. This composition is compatible with those from mafic rocks or even peridotite, but with a high Na and Al. Similar compositions also have been described from alkaline basic rocks. A calculation based on distribution of Al between pyroxene and liquid (Maurel & Maurel 1982,

TABLE 6. SELECTED ELECTRON-MICROPROBE DATA AND STRUCTURAL FORMULA OF SILICATES INCLUDED IN ISOFERROPLATINUM NUGGETS

|                                | Cpx   |       | K feld. | Albite | Amphibole |       |       |       |
|--------------------------------|-------|-------|---------|--------|-----------|-------|-------|-------|
|                                | 37.90 | 42.07 |         |        | 41.34     | 39.42 | 38.85 |       |
| SiO <sub>2</sub>               | 50.75 | 66.27 | 68.60   | 5.62   | 5.27      | 4.47  | 4.67  | 5.52  |
| TiO <sub>2</sub>               | 1.09  | 0.02  | 0.05    | 13.58  | 12.19     | 12.42 | 14.07 | 14.47 |
| Al <sub>2</sub> O <sub>3</sub> | 4.27  | 18.31 | 19.66   | -      | 0.99      | 0.86  | 0.06  | 0.08  |
| Cr <sub>2</sub> O <sub>3</sub> | 0.19  | -     | -       | -      | -         | -     | -     | -     |
| Fe <sub>2</sub> O <sub>3</sub> | -     | 0.19  | 0.01    | -      | -         | -     | -     | -     |
| FeO                            | 6.31  | -     | -       | 16.15  | 11.11     | 11.29 | 16.40 | 13.63 |
| MnO                            | 0.18  | 0.06  | -       | 0.27   | -         | 0.20  | 0.26  | 0.14  |
| MgO                            | 15.17 | -     | 0.02    | 8.87   | 11.01     | 12.07 | 8.15  | 8.60  |
| CaO                            | 20.56 | 0.08  | 0.27    | 10.95  | 10.58     | 10.95 | 11.58 | 11.39 |
| Na <sub>2</sub> O              | 0.56  | 2.84  | 11.26   | 3.28   | 2.98      | 3.14  | 2.64  | 3.03  |
| K <sub>2</sub> O               | -     | 11.78 | 0.15    | 0.64   | 0.84      | 0.80  | 0.47  | 0.80  |
| NiO                            | 0.11  | 0.07  | 0.17    | 0.02   | 0.04      | 0.04  | 0.15  | 0.02  |
| H <sub>2</sub> O               | -     | -     | -       | 1.96   | 2.02      | 2.02  | 1.98  | 1.98  |
| Tot.                           | 99.19 | 99.62 | 100.19  | 99.24  | 99.10     | 99.60 | 99.85 | 98.51 |
| Si                             | 1.88  | 12.08 | 11.96   | 5.79   | 6.23      | 6.12  | 5.96  | 5.89  |
| Ti                             | 0.03  | -     | 0.01    | 0.65   | 0.59      | 0.50  | 0.53  | 0.63  |
| Al                             | 0.19  | 3.93  | 4.04    | 2.45   | 2.13      | 2.17  | 2.51  | 2.59  |
| Cr                             | 0.01  | -     | -       | -      | 0.12      | 0.10  | 0.01  | 0.01  |
| Fe <sup>3+</sup>               | -     | 0.03  | -       | -      | -         | -     | -     | -     |
| Fe <sup>2+</sup>               | 0.20  | -     | -       | 2.06   | 1.38      | 1.40  | 2.07  | 1.73  |
| Mn                             | 0.01  | 0.01  | -       | 0.03   | -         | 0.03  | 0.03  | 0.02  |
| Mg                             | 0.84  | -     | 0.01    | 2.02   | 2.43      | 2.67  | 1.84  | 1.94  |
| Ca                             | 0.82  | 0.02  | 0.05    | 1.79   | 1.81      | 1.76  | 1.93  | 2.04  |
| Na                             | 0.04  | 1.00  | 3.81    | 0.97   | 0.86      | 0.90  | 0.77  | 0.89  |
| K                              | -     | 2.74  | 0.03    | 0.13   | 0.16      | 0.15  | 0.09  | 0.13  |
| Ni                             | -     | 0.01  | 0.02    | -      | -         | -     | 0.02  | -     |
| OH                             | -     | -     | -       | 2.00   | 2.00      | 2.00  | 2.00  | 2.00  |
| Tot.                           | 4.02  | 19.82 | 19.93   | 17.89  | 17.71     | 17.80 | 17.76 | 17.89 |

Johan & Augé 1986) indicates that it could have crystallized from a liquid with about 19 wt.%  $\text{Al}_2\text{O}_3$ .

*K-feldspar* (Table 6), either included in the isoferroplatinum alloy or embedded in PGM laths in the composite nugget, shows a similar composition ( $\text{Or}_{70}\text{Ab}_{29}\text{An}_1$  and  $\text{Or}_{71}\text{Ab}_{25}\text{An}_4$ , respectively). *Na-feldspar* (Table 6) included in isoferroplatinum nuggets appears to be close to pure albite ( $\text{Or}_1\text{Ab}_{97}\text{An}_2$ ). Nixon *et al.* (1990) interpreted similar inclusions of albite as a product of the subsolidus re-equilibration of an originally more calcic plagioclase. Obviously, a magmatic origin of such a composition is not compatible with the composition of coexisting pyroxene.

The amphibole is a Ti-rich hornblende (kaersutite), with a relatively homogeneous composition (Table 6, Fig. 14). However, chromium (0.8 to 1.0 wt.%  $\text{Cr}_2\text{O}_3$ ) appears in two grains of amphibole (one from a glass inclusion, and the other from the amphibole-pyroxene association). Cr-bearing kaersutite has a higher  $\text{Mg}/(\text{Mg}+\text{Fe})$  value (0.65, whereas it is about 0.5 for other crystals, Fig. 15). This difference confirms that Cr-bearing amphibole has crystallized from a less differentiated liquid and indicates equilibrium between pyroxene and the Cr-Mg-rich amphibole.

The  $\text{Na}/(\text{Na}+\text{K})$  ratio of the kaersutite is constant, varying between 0.8 and 0.9; its CaO content is around 10–12 wt.%. The  $\text{TiO}_2$  percentage is relatively high and constant (5–6 %); the saturation of the system in Ti is marked by appearance of Fe-Ti oxides.

The similarity in composition between amphibole associated with glass inclusions and other included grains of amphibole suggests that both have crystallized from a similar liquid. If we assume that amphibole in glass inclusions has crystallized once the melt was

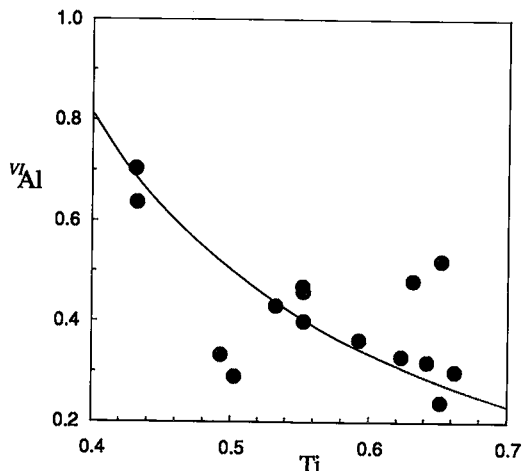


FIG. 14. Plot of  $\text{VI Al}$  versus Ti (atom %) for amphibole grains included in isoferroplatinum nuggets.

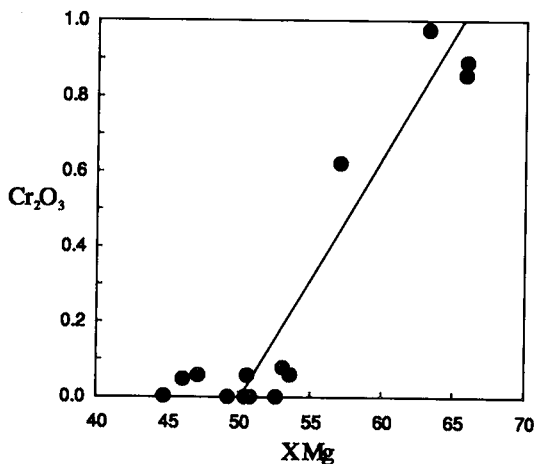


FIG. 15. Plot of  $\text{Cr}_2\text{O}_3$  (wt.%) versus  $\text{Mg}/(\text{Mg}+\text{Fe})$  (atom) for amphibole grains included in isoferroplatinum nuggets.

trapped (which is likely, since amphibole is present in all glass inclusions), we have to consider that amphibole and pyroxene not associated with glass have crystallized from a similar liquid and that glass present in the inclusion represents the residual liquid.

Raman spectra (this study) have confirmed that the Si-Al rich phase is glass. However, interpretation of its composition (Table 7) is difficult. Owing to its small size and to the presence of associated silicates, glass inclusions have been analyzed using a focussed electron beam, which makes estimation of its  $\text{H}_2\text{O}$  and alkali content difficult. Two types of composition have been obtained, both characterized by very low Ca, Fe and Mg content: a Si-rich glass ( $\text{SiO}_2$  around 80 wt.%) relatively enriched in  $\text{Al}_2\text{O}_3$  but impoverished in alkalis, and a less Si-rich glass (70–75 wt.%  $\text{SiO}_2$ ), enriched in alkalis ( $\text{Na}_2\text{O} + \text{K}_2\text{O}$  vary from 4 to 10 wt.%). The low Fe content could be due to migration of this element into the host Pt-Fe alloy.

Within a single inclusion, the composition of the glass varies largely, especially in Na/K ratio. This heterogeneity could be due to local alteration or to element migration during analysis. The best analytical total obtained for alkali-rich glass is 98% and for alkali-poor glass, 99%.

Johan *et al.* (1990) described globules of silicate glass included in Pt-Fe alloys from the Durance River. They interpreted the glass compositions as indicating an andesite to shoshonite suite. Similarly, Johan *et al.* (1991) interpreted silicate inclusions in PGE nuggets from the Fifield Alaskan-type complex as indicative of a high partial pressure of water in the melt from which the nuggets crystallized.

TABLE 7. SELECTED ELECTRON-MICROPROBE DATA OF GLASS INCLUSIONS IN ISOFERROPLATINUM NUGGETS

|                                | 1     | 2     | 3     | 4     | 5     | 6     |
|--------------------------------|-------|-------|-------|-------|-------|-------|
| SiO <sub>2</sub>               | 61.99 | 69.07 | 70.63 | 73.11 | 79.46 | 80.51 |
| TiO <sub>2</sub>               | -     | 0.04  | 0.02  | -     | 0.01  | 0.07  |
| Al <sub>2</sub> O <sub>3</sub> | 14.87 | 14.39 | 16.84 | 16.62 | 15.94 | 16.37 |
| Cr <sub>2</sub> O <sub>3</sub> | -     | 0.04  | 0.19  | 0.02  | 0.03  | -     |
| FeO                            | 1.18  | 0.23  | 0.18  | 0.04  | 0.08  | -     |
| MnO                            | 0.02  | -     | 0.02  | -     | -     | -     |
| MgO                            | 0.05  | 0.05  | -     | -     | -     | 0.06  |
| CaO                            | 0.13  | 4.74  | 0.37  | 0.40  | 0.44  | 0.31  |
| Na <sub>2</sub> O              | 0.08  | 6.45  | 7.73  | 2.72  | 0.74  | 0.39  |
| K <sub>2</sub> O               | 10.95 | 0.18  | 0.20  | 4.27  | 0.88  | 0.66  |
| NiO                            | 0.03  | -     | 0.12  | 0.04  | -     | -     |
| Tot.                           | 89.30 | 95.19 | 96.30 | 97.22 | 97.58 | 98.37 |

## DISCUSSION

One of the aims of this work was to understand the conditions of formation of the nuggets. Two possibilities can be envisaged: (1) nuggets are of a primary origin *i.e.*, resulting from high-temperature processes (magmatic, Cabri & Harris 1975, Nixon *et al.* 1990); (2) nuggets are of a secondary origin, *i.e.*, related to low-temperature alteration processes such as lateritization (Ottemann & Augustithis 1967, Bowles 1986, 1990, Burgath 1988). In both cases, leaching of the nuggets during transport also has been proposed (Cousins & Kinloch 1976). In order to solve the problem of the origin of the nuggets, four arguments can be used: (1) the form and size of the nuggets, (2) their composition, (3) the characteristics of the included PGM, and (4) the characteristics of the included silicates.

Isoferroplatinum nuggets described in this study are large (up to 1 mm) and generally rounded; they do not differ from alluvial PGM described in other placers (*e.g.*, Cousins & Kinloch 1976). The gap in size between nuggets and the platinum-group minerals found in the rocks from which nuggets are supposed to derive has been used to favor the hypothesis of a secondary origin of the nuggets (Ottemann & Augustithis 1967). Similarly, the rounded or subrounded form of the nuggets could indicate abrasion or dissolution and reprecipitation of the PGE. If the argument of size difference is now rejected (Nixon *et al.* 1990), the observation made here of high-temperature inclusions (in one case laurite, and in the other, composite globules) in the rim of nuggets precludes a low-temperature origin for the rim and suggests that nuggets have not evolved after their formation and have probably undergone only a limited transport. The rounded shape of the nuggets suggests crystallization from a medium formerly liquid. The distribution of the inclusions indicates that the nuggets have not undergone substantial secondary evolution, such as through dissolution or abrasion.

Similarly, the composition of the nuggets is compatible with a primary high-temperature origin. The most convincing argument is that the isoferroplatinum composition is related to the nature and composition of the included PGM. For example, the Pd-rich nuggets will also contain inclusions of Pd minerals. Again, presence of exsolution lamellae or blebs (of osmium or Pt<sub>3</sub>Cu) necessarily involves incorporation at high temperature of Os or Cu in the isoferroplatinum structure, which exsolved during cooling.

The diversity of the PGM included in the nuggets and the presence of the complex globules that must be explained by trapping of a droplet (*i.e.*, liquid phase) of PGE-S-Te composition confirm the high-temperature origin of the nuggets, the upper limit being fixed by the condition of stability of the amphibole. Finally, the presence of high-temperature silicates and of glass inclusions indicates that the nuggets have crystallized in a magmatic environment.

All the nuggets encountered in the concentrates consist of Pt-Fe alloy, although a sampling bias is possible. The composition of the nuggets is variable, but close to Pt<sub>3</sub>Fe. This suggests a common origin for all the nuggets and could indicate relatively uniform conditions during crystallization (*e.g.*, constant oxygen fugacity). In detail, variations in the composition of the isoferroplatinum is defined by substitution of Fe for Cu and of Pt for other PGE, probably reflecting local changes in the composition of the medium from which they derive. Pt is the dominant PGE.

The most common inclusions found in isoferroplatinum nuggets consist of an Os-rich Os-Ir alloy. We consider that their origin relates to two different processes: (1) exsolution, and (2) entrapment of minerals. The former corresponds to the very thin lamellae oriented in the host crystal (similar to those shown by Cabri *et al.* 1981, Fig. 14), and the latter, much more common here, to laths in the nuggets (see Fig. 2E). Such laths of Os-Ir crystals are generally interpreted as exsolution-related (Toma & Murphy 1977, Törnroos & Vuorelainen 1987, Slansky *et al.* 1991). However, the Os-Ir alloy is preferentially found in Ir-Os-rich isoferroplatinum nuggets. Thus, we consider that the presence of the laths, together with the Os-Ir enrichment in isoferroplatinum, indicate crystallization from a medium enriched in these elements; only the laths oriented in the host nugget are the result of an exsolution process. The same phenomenon is invoked for Ru and laurite.

Our study of the paragenesis of the PGM included in the nugget permits us to propose the following sequence of crystallization. First, Os-Ir alloy (or Ir oxide) crystallizes, followed by Os alloy, followed by PGE sulfide, laurite being the first sulfide to appear. At this stage, immiscible droplets of a Pt-Pd-Rh-Cu-Ir-Te sulfide liquid were formed. Finally, the whole paragenesis is trapped by isoferroplatinum crystallization.

Concerning the composition of the included minerals, the absence of Ni-bearing minerals, the very low content

of Ni in PGM, and the absence of base-metal sulfides should be emphasized. The relative Os-enrichment observed for alloy compared to alloy described as inclusion in Pt-Fe nuggets from other placers could be explained by different conditions of crystallization, as suggested here by the presence of iridium oxide.

The presence of glass of rhyolitic composition trapped in isoferroplatinum nuggets is surprising but not uncommon. Similar silicate-glass inclusions (with, in some cases, comparable composition) have been described in similar nuggets of platinum (Johan *et al.* 1990, 1991). The compositions obtained here for silicate and glass inclusions, with on the one hand mafic minerals (Mg-Cr-bearing pyroxene and amphibole, considered to have crystallized from a mafic magma), and on the other, Na-K-Si-rich glass and minerals (feldspars), are surprising. We suggest that they reflect the presence, at a certain stage, of two magmas of different composition. However, amphibole coexists with these two compositions; Cr-Mg-rich kaersutite, associated with Cr-rich pyroxene, are considered to have crystallized from the basic magma, and Mg-poor amphibole, found with glass inclusion, to have crystallized from the felsic magma. The association of a relatively evolved and a basic paragenesis has already been mentioned. Nixon *et al.* (1990) described an ultramafic paragenesis consisting of chromite and olivine supposedly contemporaneous with high-temperature crystallization of the nuggets and a more evolved paragenesis consisting of albite, iron-rich clinopyroxene, pargasite, phlogopite and biotite. This latter association is interpreted as the result of fractionation of a primitive melt trapped in the nuggets at the time of chromite formation. However, for the example of the Madagascar nuggets, we have to consider three alternative hypotheses. The first is that phases associated with amphibole (*i.e.*, pyroxene, Fe-Ti oxide and glass) correspond to the melting of amphibole. This possibility, however, is difficult to accept, in view of the composition and proportion of the glass. The second is that the felsic composition corresponds to a residual liquid after fractional crystallization, but the proportion of glass inclusions and the composition of the glass do not argue in favor of the hypothesis. The third hypothesis involves a model of the coexistence of two different magmatic liquids, felsic and basic (Cr-bearing). Two mechanisms can lead to the coexistence of these two liquids (1) immiscibility (due to particular conditions of the evolution of the magma), and (2) magma mixing (due to contamination, for example).

The close association of the nuggets with representative end-members magmas having different compositions suggests that PGM formation could be, to a certain extent, connected with this phenomenon of coexistence of the two different magmas. We suggest that source of PGE would be the primitive magma; the role of the evolved liquid would be to provoke local oversaturation in PGE. However, contrary to the models developed in other contexts (*e.g.*, Campbell *et al.* 1983,

Naldrett *et al.* 1990), we do not have evidence here of the role played by a sulfide phase in PGE concentration.

One of the most striking observations concerning the isoferroplatinum nuggets in placers is the similarity in the observations made worldwide in geological contexts that are not similar *a priori*. The presence of osmium laths has been known for a long time, but the more recent papers describe a complex paragenesis of included PGM and silicates comparable to that observed here. Note particularly that the first occurrences of kashinite and vinentite have been discovered in a similar context (Begizov *et al.* 1985, Stumpfl & Tarkian 1974). Although in three cases the isoferroplatinum nuggets have been clearly established to derive from Alaskan-type complexes [Zhdanov & Rudashevskii (1980) and Rudashevskii & Zhdanov (1983) for an intrusion in Kamchatka (see Johan *et al.* 1990), Nixon *et al.* (1990) for the Tulameen complex, and Johan *et al.* (1991) for the Fifield complex], minor but perhaps important differences appear from one context to the other. For example, Johan *et al.* (1991) emphasized the lack of laurite, and Nixon *et al.* (1990) pointed out the nature of alloys of Pt-Fe-Cu-Ni. Thus, one must wonder if this type of PGE nugget is characteristic of the type of source, such as an Alaskan-type complex.

If the answer to this question is positive, it would imply generalization to other environments where the geological context is poorly known, such as for Madagascar. On the basis of mineralogical analogies, Johan *et al.* (1990) concluded that the PGM discovered in the Durance River (France) probably derive from an Alaskan-type intrusion. In spite of the fact, as pointed out by Johan *et al.* (1990), that such an association of PGM is very characteristic of Alaskan-type intrusions, we consider that there is not yet enough information to permit these generalizations and suggest this theme as a direction for further work. The discovery of primary PGE mineralization in Alaskan-type complexes (Johan *et al.* 1989, Nixon *et al.* 1990) makes this type of investigation promising.

## CONCLUSION

Isoferroplatinum nuggets found in the Antanambao-Manampotsy area, eastern Madagascar, have characteristics similar to those from other placers. Silicates and glass inclusions within the nuggets indicate that they have formed at magmatic conditions and have undergone very little secondary evolution. They derive from a medium enriched in Pt, with variable amounts of other PGE, reflected by the nature of included PGM in the nuggets and by the nuggets' composition.

Absence of base-metal sulfides and the scarcity of PGE sulfides compared to alloys denote a low fugacity of sulfur.

The nature of silicate and glass inclusions contained in the nuggets suggests that isoferroplatinum crystallization could have been influenced by the coexistence

of two different magmas. Alaskan-type complexes are a type of source that has to be envisaged for these nuggets.

#### ACKNOWLEDGEMENTS

This work has been undertaken within the framework of an EEC project on PGE mineralization (contract number MA1M - 0008 - F[CD]). We thank M. Kerjean, who very kindly gave us the concentrates, C. Gilles for carrying out the electron-microprobe analyses, J. Breton for the SEM images, F. El Kaliobi for image analyses, and C. Beny for the Raman probe results. We are grateful to Z. Johan, M. Ohnenstetter, Y. Moëlo, M. Pichavant and D. Watkinson for fruitful discussions. The last named is also especially thanked for improving the English of the manuscript. R.F. Martin is thanked for his editorial comments, and G.T. Nixon and G.A. Desborough for useful reviews.

#### REFERENCES

- AUGÉ, T. (1988): Platinum-group minerals in the Tiébaghi and Vourinos ophiolitic complexes: genetic implications. *Can. Mineral.* **26**, 177-192.
- \_\_\_\_\_ & JOHAN, Z. (1988): Comparative study of chromite deposits from Troodos, Vourinos, North Oman and New Caledonia ophiolites. In *Mineral Deposits within the European Community* (J. Boissonas & P. Omenetto, eds.). Springer-Verlag, Berlin (267-288).
- BEGIZOV, V.D., ZAVYALOV, E.N., RUDACHEVSKII, N.S. & VYALSOV, L.N. (1985): Kashinite (Ir,Rh)<sub>2</sub>S<sub>3</sub> - a new iridium and rhodium sulfide. *Zap. Vses. Mineral. Obshchest.* **114**, 617-622 (in Russ.).
- BOWLES, J.F.W. (1981): The distinctive suite of platinum-group minerals from Guma Water, Sierra Leone. *Bull. Minéral.* **104**, 478-483.
- \_\_\_\_\_ (1986): The development of platinum-group minerals in laterites. *Econ. Geol.* **81**, 1278-1285.
- \_\_\_\_\_ (1990): Platinum-iron alloys, their structural and magnetic characteristics in relation to hydrothermal and low-temperature genesis. *Mineral. Petrol.* **43**, 37-47.
- BURGATH, K.P. (1988): Platinum-group minerals in ophiolitic chromitites and alluvial placers deposits, Meratus-Bobaris area, southeast Kalimantan. In *Geo-Platinum, Proc. Symp. Geo-Platinum 87* (H.M. Prichard, P.J. Potts, J.F.W. Bowles & S.J. Cribb, eds.). Elsevier, New York (383-403).
- CABRI, L.J., CRIDDLE, A.J., LAFLAMME, J.H.G., BEARNE, G.S. & HARRIS, D.C. (1981): Mineralogical study of complex Pt-Fe nuggets from Ethiopia. *Bull. Minéral.* **104**, 508-525.
- \_\_\_\_\_ & FEATHER, C.E. (1975): Platinum-iron alloys: a nomenclature based on a study of natural and synthetic alloys. *Can. Mineral.* **13**, 117-126.
- \_\_\_\_\_ & HARRIS, D.C. (1975): Zoning in Os-Ir alloys and the relation of the geological and tectonic environment of the source rocks to the bulk Pt:Pt+Ir+Os ratio for placers. *Can. Mineral.* **13**, 266-274.
- \_\_\_\_\_, LAFLAMME, J.H.G., STEWART, J.M., TURNER, K. & SKINNER, B.J. (1978): On cooperite, braggite, and vysotskite. *Am. Mineral.* **63**, 832-839.
- \_\_\_\_\_, ROWLAND, J.F., LAFLAMME, J.H.G. & STEWART, J.M. (1979): Keithconnite, telluropalladinite and other Pd-Pt tellurides from the Stillwater complex, Montana. *Can. Mineral.* **17**, 589-594.
- CAMPBELL, I.H., NALDRETT, A.J. & BARNES, S.J. (1983): A model for the origin of the platinum-rich sulfide horizons in the Bushveld and Stillwater complexes. *J. Petrol.* **24**, 133-165.
- CONRAUX, J. (1962): *Antanambao-Manampotsy*. BRGM, Orléans, France (unpubl. rep.).
- COUSINS, C.A. & KINLOCH, E.D. (1976): Some observations on textures and inclusions in alluvial platinoids. *Econ. Geol.* **71**, 1377-1398.
- CRIDDLE, A.J. & STANLEY, C.J. (1985): Characteristic optical data for cooperite, braggite and vysotskite. *Can. Mineral.* **23**, 149-162.
- FEATHER, C.E. (1976): Mineralogy of platinum-group minerals in the Witwatersrand, South Africa. *Econ. Geol.* **71**, 1399-1428.
- HANSEN, M. & ANDERKO, K. (1958): *Constitution of Binary Alloys*. McGraw-Hill, New York.
- HARRIS, D.C. & CABRI, L.J. (1973): The nomenclature of natural alloys of osmium, iridium and ruthenium based on new compositional data of alloys from world-wide occurrences. *Can. Mineral.* **12**, 104-112.
- \_\_\_\_\_ & \_\_\_\_\_ (1991): Nomenclature of platinum-group-element alloys: review and revision. *Can. Mineral.* **29**, 231-237.
- HENRY, B. (1962): *Mission Cote Est Anosibe*. BRGM Orléans, France (unpubl. rep.).
- JOHAN, Z. & AUGÉ, T. (1986): Ophiolitic mantle sequences and their evolution: mineral chemistry constraints. In *Metallogeny of Basic and Ultrabasic Rocks* (M.J. Gallagher, R.A. Ixer, C.R. Neary & H.M. Prichard, eds.). Institution of Mining and Metallurgy, London (305-317).
- \_\_\_\_\_, OHNENSTETTER, M., FISCHER, W. & AMOSSÉ, J. (1990): Platinum-group minerals from the Durance River alluvium, France. *Mineral. Petrol.* **42**, 287-306.
- \_\_\_\_\_, \_\_\_\_\_, SLANSKY, E., BARRON, L.M. & SUPPEL, D. (1989): Platinum mineralization in the Alaskan-type intrusive complexes near Fifield, New South Wales, Australia. 1. Platinum-group minerals in clinopyroxenites of the Kelvin Grove Prospect, Owendale intrusion. *Mineral. Petrol.* **40**, 289-309.

- , SLANSKY, E. & OHNENSTETTER, M. (1991): Isoferroplatinum nuggets from Milverton (Fifield, N.S.W., Australia): a contribution to the origin of PGE mineralization in Alaskan-type complexes. *C.R. Acad. Sci. Paris, Sér. II*, **312**, 55-60.
- KIM, WON-SA, CHAO, G.Y. & CABRI, L.J. (1990): Phase relations in the Pd-Te system. *J. Less-Common Metals* **162**, 61-74.
- LEGENDE, O. (1982): *Minéralogie et géochimie des platinodes dans les chromites ophiolitiques: comparaison avec d'autres types de concentrations en platinoïdes*. Thèse de doctorat de 3ème cycle, Université P. et M. Curie, Paris.
- (1990): A possible epitaxy of laurite on rutheniridosmine from ophiolitic chromitite: genetic implications. *Int. Mineral. Assoc., Gen. Meet. (Beijing), Abstr. 1*, 259-260.
- & AUGÉ, T. (1986): Mineralogy of platinum-group mineral inclusions in chromitites from different ophiolitic complexes. In *Metallogeny of Basic and Ultrabasic Rocks* (M.J. Gallagher, R.A. Ixer, C.R. Neary & H.M. Prichard, eds.). Institution of Mining and Metallurgy, London (361-372).
- MAUREL, C. & MAUREL, P. (1982): Etude expérimentale de la distribution de l'aluminium entre bain silicaté basique et spinelle chromifère. Implications pétrogénétiques: teneur en chrome des spinelles. *Bull. Minéral.* **105**, 197-202.
- NALDRETT, A.J., BRÜGMANN, G.E. & WILSON, A.H. (1990): Models for the concentration of PGE in layered intrusions. *Can. Mineral.* **28**, 389-408.
- NIXON, G.T., CABRI, L.J. & LAFLAMME, J.H.G. (1990): Platinum-group element mineralization in lode and placer deposits associated with the Tulameen Alaskan-type complex, British Columbia. *Can. Mineral.* **28**, 503-535.
- OTTEMANN, J. & AUGUSTITTHIS, S.S. (1967): Geochemistry and origin of "platinum-nuggets" in lateritic covers from ultrabasic rocks and birbrites from W. Ethiopia. *Mineral. Deposita* **1**, 269-277.
- RUDASHEVSKII, N.S. & ZHDANOV, V.V. (1983): Accessory platinum mineralization within a mafic-ultramafic intrusion in Kamchatka. *Bull. Mosk. Obschest. Izpyt. Prirody Otd. Geol.* **58**, 49-59 (in Russ.).
- SLANSKY, E., JOHAN, Z., OHNENSTETTER, M., BARRON, L.M. & SUPPEL, D. (1991): Platinum mineralization in the Alaskan-type intrusive complexes near Fifield, N.S.W., Australia. 2. Platinum-group minerals in placer deposits at Fifield. *Mineral. Petrol.* **43**, 161-180.
- STUMPFL, E.F. & TARKIAN, M. (1974): Vincentite, a new palladium mineral from south-east Borneo. *Mineral. Mag.* **39**, 525-527.
- TARKIAN, M. (1987): Compositional variations and reflectance of common platinum-group minerals. *Mineral. Petrol.* **36**, 169-190.
- TOMA, S.A. & MURPHY, S. (1977): The composition and properties of some native platinum concentrates from different localities. *Can. Mineral.* **15**, 59-69.
- TÖRNROOS, R. & VUORELAINEN, Y. (1987): Platinum-group metals and their alloys in nuggets from alluvial deposits in Finnish Lapland. *Lithos* **20**, 491-500.
- ZHDANOV, V.V. & RUDASHEVSKII, N.S. (1980): New type of Pt-Au mineralization in metasomatites after mafic rocks. *Dokl. Akad. Nauk SSSR* **252**, 1452-1456 (in Russ.).

Received May 24, 1991, revised manuscript accepted February 19, 1992.